UNIVERSIDAD AUTÓNOMA DE SAN LUIS POTOSÍ

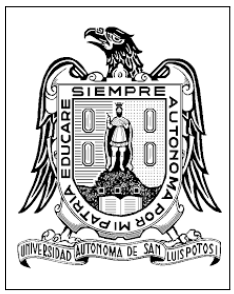

Comparative study of dynamical and structural properties of two eutectic solvents, using molecular dynamics simulation

TESIS

QUE PARA OBTENER EL TÍTULO DE MAESTRO EN CIENCIAS (FÍSICA)

PRESENTA

RODRIGO RODRÍGUEZ GUTIÉRREZ

ASESOR: DR. MAGDALENO MEDINA NOYOLA

COASESOR: DR. PEDRO EZEQUIEL RAMÍREZ GONZÁLEZ

SAN LUIS POTOSÍ, S.L.P. 30 DE SEPTIEMBRE DE 2019

Acknowledgments

I want to thank Dr. Magdaleno Medina Noyola and Dr. Pedro Ezequiel Ramírez González for advising me in the achievement of this project, also Dr. Gan Ren of the Institute of theoretical Physics of Chinese academy of science for providing support in the beginning of the project, and the LANIMFE staff for their advise and friendship.

I also want to thank the support of my examination committee composed by Dr. Martín Chavéz Páez, Dr. José Elías Pérez López and Dr. Enrique González Tovar for taking the time to review my thesis. Also to the staff of the IF (Instituto de Física), in particular to J. Limón Castillo for the computational support.

This project would not be possible without the support of my friends and teachers, that made my stay in the university more gratifying, and my family and close friends that motivated and encouraged me to work hard every day.

I want to thank to CONACyT (Consejo Nacional de Ciencia y Tecnología) for the administrative support, and for giving me the honor of granting me the scholarship No. 476638 with the register No. 628178 and through Grant No. CB-2015-2-257636. Also to LANIMFE (Laboratorio Nacional de Ingeniería de la Materia Fuera del Equilibrio) for the technical and computational support.

. . . a mi abuelita Agustina Ruíz Huerta .

Contents

List of Figures

List of Tables

1 Introduction

Current times are known as the digital era. Almost all the rutinary devices are controlled by some kind of electronic system. We are embedded in a world dominated by electronics, robotics and telecommunications. Actually, the society are entering in a huge change, where the digitalization of economy, manufacturing and even social relations, represents the next technological horizon. Beyond the next technological frontier, we expect smart houses, intelligent buildings and autonomous cars, with the capacity of monitorate by itself and use artificial intelligence algorithms for taking data enhanced decisions, improving the security and providing an efficient utilization of resources.

Such a digital world works with electricity. Thus, we need vast, efficient and clean forms to generate enough power. Recently, technologies as the solar or eolic generation are becoming very popular as clean and efficient energy sources.

One of the most important pieces in all this digital era is the energy storage. Anyone of the electronic devices used by the people, or by the clean energy generation systems, are useful without an electricity storage system, i.e., they needs a battery.
There exists many forms to design a battery. However, the current designs are very close to their limits. Hence, the research in compounds with conductive capacity has been of great interest in recent years. Among such kind of systems, the so-called Room-Temperature Molten Salts, or simply Ionic Liquids (ILs), and the Deep-Eutectic Solvents (DES), have been widely studied in the last forty years. The ILs are usually formed by organic ions and have the property of being liquids at temperatures below 100 $^{\circ}C$. The DES are essentially an IL in which a third (non-charged) compound, usually called the hydrogen-bond donor, is introduced. The addition of the hydrogen-bond donor changes enormously the properties of

the solvent, compared with the behavior of each of the compounds in their pure state. Such kind of compounds are becoming very popular in recent years due to they promising applications in industry, in particular in battery manufacturing.
Despite the intense investigation in these liquids, many of their most essential features are still matter of debate. For example, the physical reason because such compounds are liquid at room temperature is not fully understood.

In this work we analyzed the dynamical and structural properties of two eutectic solvents using molecular dynamic simulations, this was done to understand the behavior of the two eutectic solvents in contrast with Ionic Liquids. The main aim is to obtain physical insights that explains the decreasing of the freezing point in DES.

The dynamical and structural analysis consist on the radial distribution function and mean square displacement. In addition, thermochemical analysis of the crystalline structure of the compounds was made .

In order to obtain a better understanding of the decreasing of the freezing point in ILs and DES, we focus in two principal issues. The first one is the long-range interaction behavior, associated with the Coulomb potential and the other is the short range interaction, associated with the package effect related to the size of the particles.

A simplified model of the two eutectic solvents was proposed using as inputs the effective ionic diameter of the ions σ and the dielectric constant ϵ.

2 Background

Recently, deep eutectic solvents have captured a lot of attention of the scientific community [26][25].
Primordially due to the encouraging industrial applications and its potential of substituying organic solvents. Similar to room-temperature ionic liquids [26][25], eutectic solvents are considered green solvents principally because of their easy recovery and recycling into industrial processes.

Let us start explaining the definition of deep eutectic solvent (DES) and highlight their importance and the relevant problems around such kind of liquids.

The word eutectic comes from the Greek and means easy melting. Thus, the term refers to a compound which has a facility to melt.
An eutectic mixture, is a mixture that has a lower freezing point that their constituents, generally mixing two solid compounds to form a liquid mixture [26][25].

Eutectic solvents are formed by a salt, generally a Quaternary ammonium salt and a Hydrogen bond donor (HBD), the HBD can be a carboxilic acid, amide, polyol or an amino acid [26][25].

Currently eutectic solvents rise as an alternative to the so called room-temperature ionic liquids or simply ionic liquids (ILs), which were widely studied because their possible industrial utility, owing their low vapor pressure (sealant), high boiling point (recycling), among other interesting properties [26][25].

Usually, a DES is composed by a ionic liquid, i.e., an organic cation and an anion, combined with a third compound which acts as a hydrogen-bonds donor. Such combination results in a quite different properties compared

with a pure ILs [26][25]. It is our interest to investigate the molecular origins of such differences and try to explain them in physical terms.

Similarly to ILs, DES have amazing of possibilities due to the overwhelming number of combinations of the three components. The diversity of possible combinations implies that such solvents can be literally designed for especific applications [26][25].

Nowadays, the DES have attracted a lot of the attention of the soft matter community due their amazing potential.

One of the problems working with ILs is that you need high purity compounds in order to produce them, impliying a high cost in their fabrication.
Furthermore, reports have shown that ILs have low biodegradability, toxicity and some of them are hazardous [1][26].

For this reasons people that have been working with ILs have opted to study compounds with similar properties that ILs but environmentally friendlier, here is were the eutectic solvents join the scene with properties similar to ILs but because of the organic nature of their constituents they are less toxic and have better biodegradability than ILs [1][26].

Currently , DES have been applied in multiple areas. For instance [26][25].

Despite of the intense research around DES, a many of their most important issues still unsolved. For instance, the physical mechanism which permits the depression of the melting point of the eutectic mixture.

The principal eutectic solvents that have been studied are the mixed between choline chloride and urea, sometimes called reline. An important part in these studies have been found the molar ratio between choline chloride and urea that produces the eutectic mixed with the lowest freezing point. It have been shown experimentally that a molar ratio of 1:2 between choline chloride and urea produces the lowest freeazing point ($12°C$), this is much lower than the freezing point of choline chloride ($302°C$) and urea ($133°C$) [1].

In the present work we are interested in obtaining physical insights about this point.

The structure of the eutectic solvent compounds analyzed in the present work are shown in Figure 1.

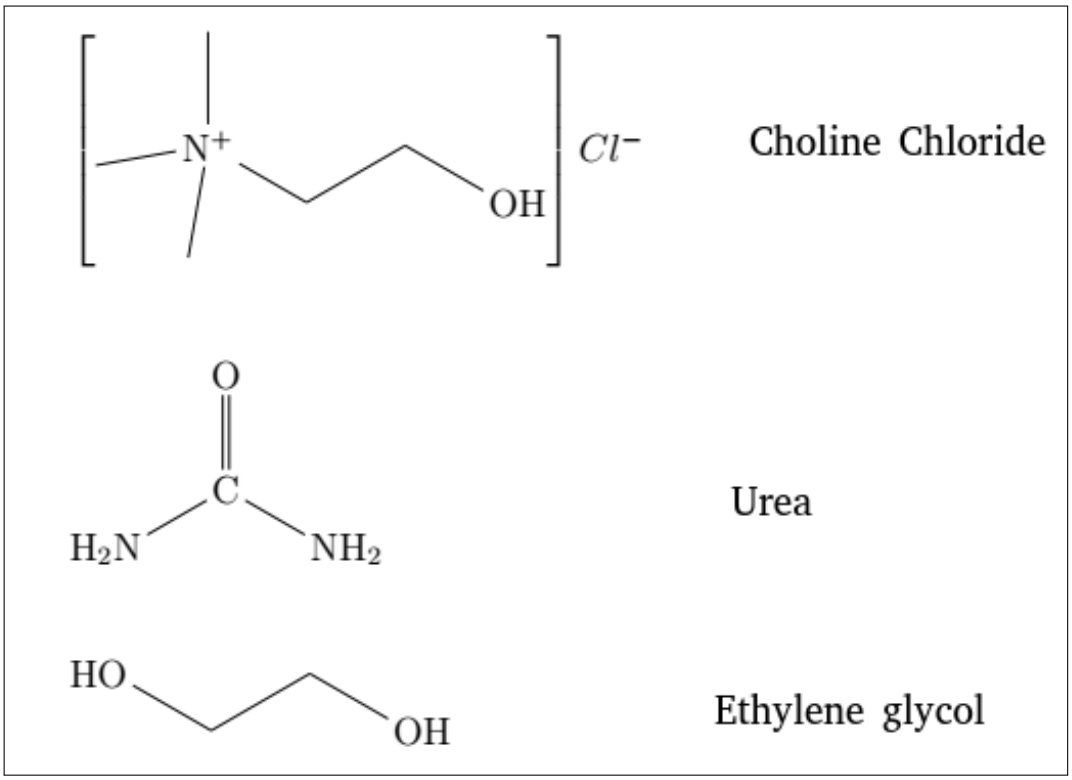

Figure 1: Structure of eutectic solvent compounds analyzed

We can observe the difference in size between the cation (choline +) and the anion (chloride -).

Another characteristics of interest in these studies are the density, conductivity and the capacity of forming glass [9].

One useful way to study eutectic solvents is using computational simulations because we can see some molecular interactions among the

compounds. Several chemical properties of eutectic solvents have been studied with the help of molecular dynamic (MD) simulations [24][21][22].

However, most of the power of the molecular dynamics studies are not explored yet. One of the main objectives of the present work is to exploit MD simulations in order to gain physical insights about the phase diagram of DES.

An important part of MD simulations is the force field parametrization which will help us to create the topology of our interest molecules. A key part in this parametrization is the charge assignment for the force field, García and coworkers made an interesting work on this topic. [12].

Simulations made with eutectic solvents at room temperature (300 k) have shown similar results regarding the decrease of the freezing point of the eutectic mixtures compared with their individual constituents.

This simulations exhibit main features related with the HBD concentration and the formation of hydrogen bonds. First, in studies with choline cloride and urea mixtures to make possible the decrease of the freezing point, we need an urea concentration about 67.7% or 1:2 molar ratio, this make the cation-anion, cation-urea and anion-urea interaction more modest and promote the formation of hydrogen bonds between the anion and the urea, and between the HBD with other HBD [24][22].

An important feature regarding the mixture between choline chloride and ethylene glycol is that, this mixture has the lowest freezing point of all the eutectic mixtures studied experimentally [26][25], so that can be a good starting point to understand how the decreasing of the freezing point occurs.

In other simulation study, choline chloride was kept in the eutectic mixtures but the HBD was change in the different mixtures to determine the effect of the HBD over the anion, the HDB used were one dicarboxilic acid which was malonic acid (-COOH group), and two monomeric polyols, ethylene glycol (two -OH groups) and glycerol (one -OH group). All the mixtures exhibited a high relative hydrogen bonding between the anion and the HBD, and in two of them (ethylene glycol and glycerol) there were

important interaction between HBD with HBD [21].

In the next table we show the freezing points of choline chloride (ChCl), Urea (Ure) and Ethylene glycol (Etg) and their mixtures.

Compound	ChCl	Ure	Etg	ChCl + Ure	ChCl + Etg
T_f / $°C$	302	134	-12.9	12	-66

Table 1: freezing points of the compounds analyzed

With this features we made a possible explanation for the decreasing of the freezing point in the eutectic mixtures, but with a different approach, more in touch with the physical aspects of the phenomena, rather than chemical properties of the compounds.

3 Methodology

3.1 System preparation

In this comparative study, we use 2 different mixtures of DES, one of them is a mixture of choline chloride with urea (ChCl-Ure), and the other choline chloride with ethylene glycol (ChCl-Etg) and an IL (ChCl).

The final md-production simulations were made at 300 k to analyze properties at room temperature.

For all our simulations we used the GROMACS MD simulation package with the Amber 94 force field.

The Choline, Urea and Ethylene glycol molecules were develop by Dr. Gan Ren in a similar way that [23], using the Amber 94 force field [8].

We needed to add just 3 angles that were not in the Amber 94 force field used by Gromacs. Those angles are shown in the next image.

```
[ angletypes ]
;  i    j    k  func       th0       cth
HC  CT  N3          1   109.500    418.400 ; ADAPTED BY PEDRO E. FOR CHOLINE
H1  CT  OH          1   109.500    418.400 ; ADAPTED BY PEDRO E. FOR CHOLINE
OH  CT  HC          1   109.500    418.400 ; ADAPTED BY RODRIGO R. FOR ETHYLENE GLYCOL
```

Figure 2: Angles added to Amber 94 force field

The steps needed to prepared the mixtures with just the key parts are shown in the next part, a detailed step by step tutorial is given in [18].

- First we create the topology for the molecules, the topology contains all the information that defines the molecule in the simulation, like bonded parameters and non-bonded parameters. GROMACS have a tool called pdb2gmx that create the topology of the system using the structure file of the molecule [2], which contains the positions of the atoms that form the molecule.

- Minimized the structure of the molecules. This is done using the steepest descendant method (Saddle point theorem) [11][2], the minimization is converged when the maximum force is smaller than a selected value.

- Prepared the mixtures using $2^8(256)$ ionic pairs for the ChCl-Ure and ChCl-Etg mixtures, in a molar ratio of (1:2) and for the ChCl salt we added $2^9(512)$ ionic pairs, in the same step we created a cubic box of 10 nm^3. To do this, we used a GROMACS tool called insert-molecules, which makes copies of the molecules and insert them in the vacant space of a box of selected size [2], the selection of the empty space is based on the Van der Waals radii [15][19] of the atoms, the insertion positions are random, taking a specified initial seed.

- Minimizing the energy of the system again, to fit the molecules in the box. This is done using the steepest descendant method, the minimization is converged when the maximum force is smaller than a selected value.

- The next step was the equilibration of the mixtures using several steps of NVT and NPT ensembles according to [23], we will describe the process and show a diagram of the followed steps.

All the simulations were made in a cubic box with periodic boundary conditions (PBC), and for the non-bonded interactions we applied a cut off of 1.6 nm.

The Particle Mesh Ewald (PME) was applied to handle the long-range electrostatics interactions. A more detailed treatment of (PME) is given by [11][2].

3.2 System equilibration

I want to start with some of the struggles that one can have simulating this eutectic solvents.

One of the characteristics of these compounds are the slow dynamics, caused by the polarity of the molecules. Hence, they need more time to be in an homogeneous state.

Another characteristic is that we need to use short time steps due to the Hydrogen bond-angle vibrations , that affect functional groups as $-OH$, $-CH$- or $-NH_3^+$ [2], which are in the molecules that we used.

Because we started with a random configuration of molecules in a system with slow dynamics, we tried to pre-prepare the system before the annealing, to reach a better homogenization.

First we carried the system into a separate NVT and NPT procedures of 0.1 ns to reach a temperature of 2000 k and a pressure of 101.325 bar(100 atm) before the annealing, this helped the system to be more homogeneous.

Then the system went to a NPT annealing with a constant pressure of 1 atm for a total time of 7 ns, from 2000 k to 300 k, the annealing temperatures and times are shown in the scheme.

The last configuration was then equilibrated with an NPT simulation at pressure of 1 atm and temperature of 300 k for 1 ns, to obtain the average box volume.

The system then went to a NVT annealing for a total time of 7 ns, from 2000 k to 300 k, the annealing temperatures and times are shown in the scheme.

The last configuration was now at 300 k and 1 atm, which are room conditions and then we could use the last configuration for the MD-production running.

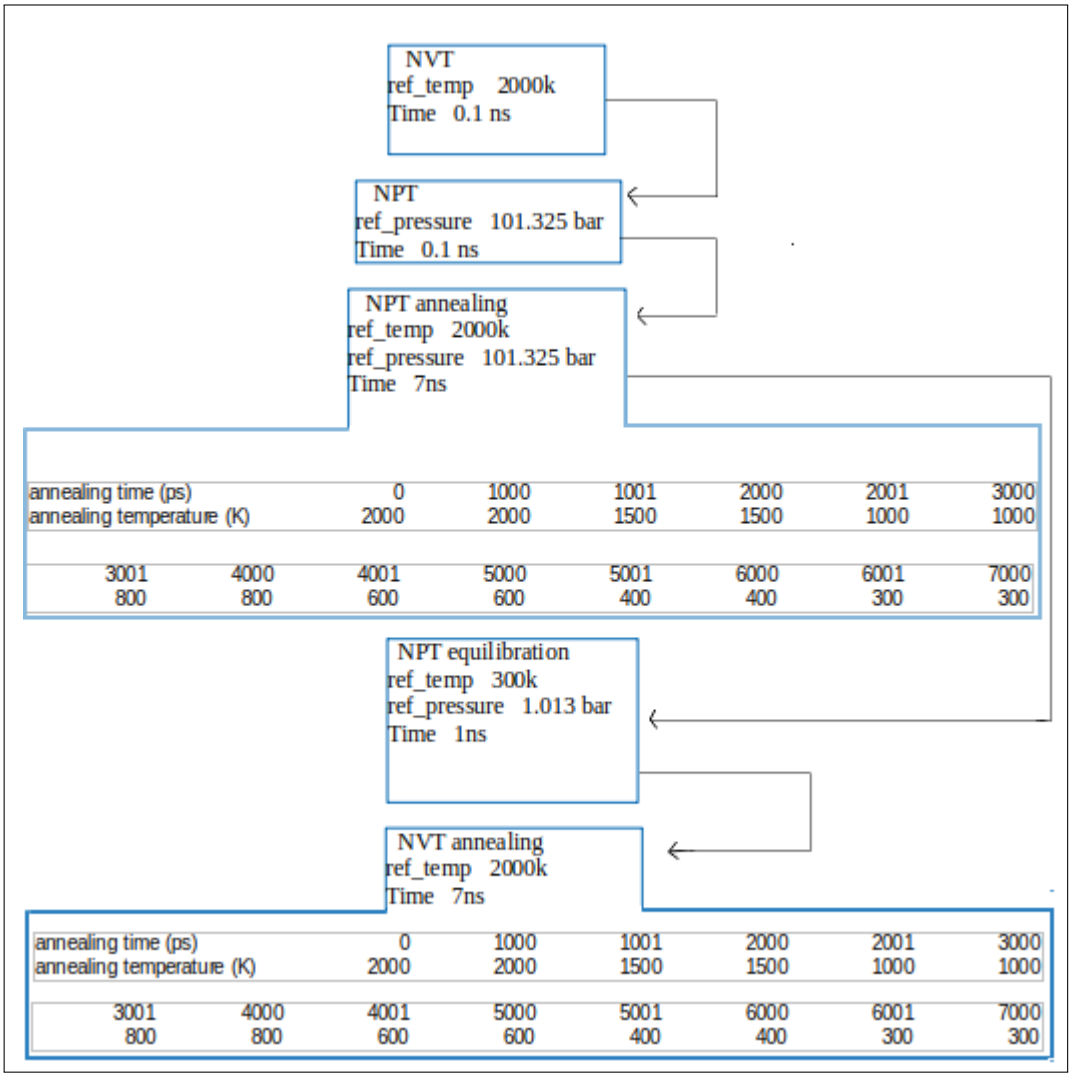

Figure 3: Equilibration

In the annealing processes of the equilibration, we monitored the volume of the boxes and the pressures of the systems. The results are shown in the next figures.

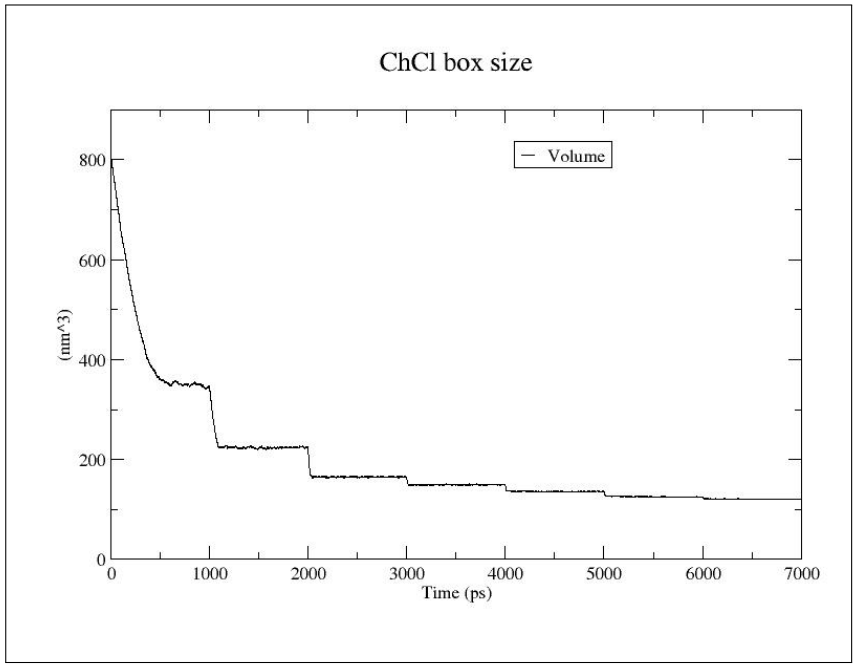

(a) NPT annealing

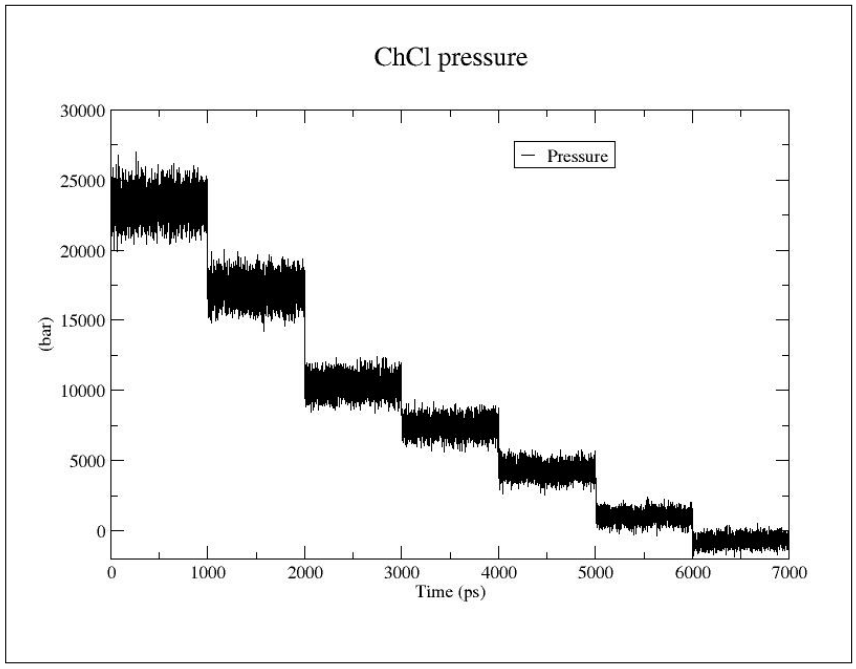

(b) NVT annealing

Figure 4: ChCl system

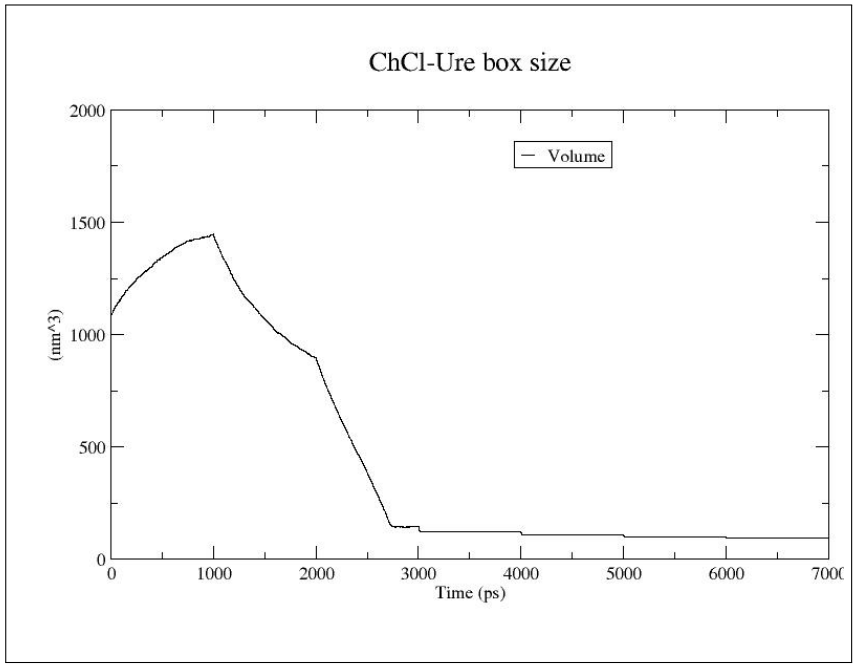

(a) NPT annealing

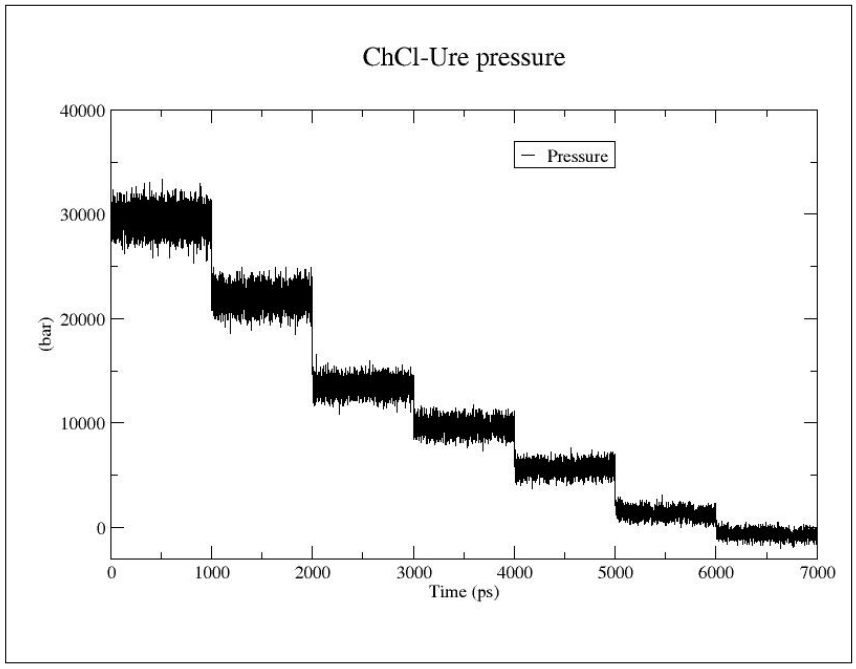

(b) NVT annealing

Figure 5: ChCl-Ure system

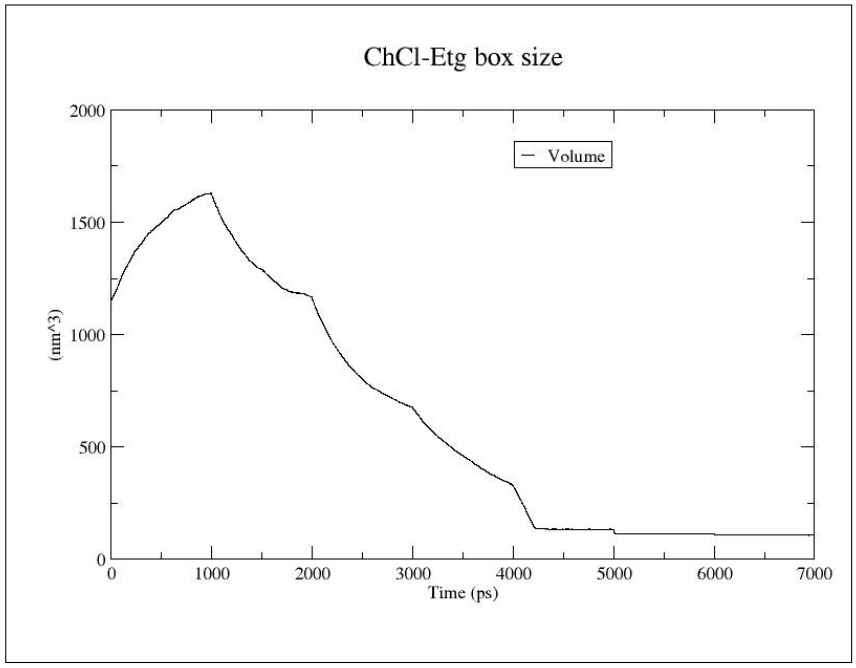

(a) NPT annealing

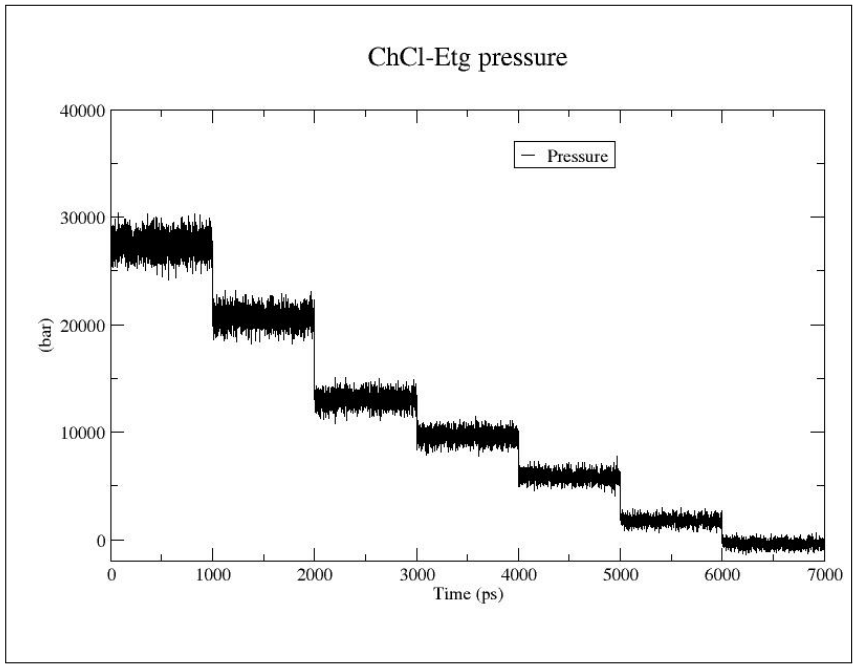

(b) NVT annealing

Figure 6: ChCl-Etg system

4 Structural and dynamical properties

In order to obtain reliable results we performed that we call production simulations. Such production simulations are performed using the most equilibrated sample (see previous chapter as starting point). Such sample is now subjected to an NVT simulation at T=300 K for 20 ns. In order to have a reference distance until useful in the interpretation of our results we estimated the effective diameter of each of the components of the system. The estimation was made with two different methods.

We calculated the radial distribution function from the center of mass of the molecules. In order to interpret correctly the information contained in the radial distribution functions, it is very convenient to make an estimation of the diameter of the molecules involved.

First we measured the diameter of the molecules taking the distance of the most distant atoms in the molecule, and assume an spherical diameter as a zero-order approximation.

We also obtain the ionic diameter for the Cl^- and Ch^+ ions, in the case of the ion choline, we made an approximation of the ionic diameter considering that in the formation of the ionic bond, the cation reduce its size while the chloride ion increase their size. The atomic and ionic diameters of sodium and chloride were obtained from [6]. The results are in the next table.

Compound	Ch	Ure	Etg	Cl	Na
Approx atomic diameter(nm)	0.5766 nm	0.3833 nm	0.4020 nm	0.198 nm	0.382 nm

Table 2: Approximate atomic diameter of the compounds analyzed

Compound	Ch	Cl	Na
Approximate ionic diameter (nm)	0.500 nm	0.362 nm	0.198 nm

Table 3: Approximate ionic diameter of the compounds analyzed

These measures were used to analyzed the results obtained in the MD-simulation.

With the aim of presenting the information in a clear manner, first the RDFs are shown with an interpretation of the graphics. The comparison among the mixtures and the interpretation of the results are given in the discussion contained in chapter 6.

In the next figures we used $g_{\alpha\beta}$ to define the radial distribution functions between different molecules. The combinations of $g_{\alpha\beta}$ are presented in the next table.

$g_{\alpha\beta}$	Interaction	symbol
g_{++}	cation-cation	CHL-CHL
g_{+-}	cation-anion	CHL-CL
g_{+U}	cation-urea	CHL-URE
g_{U-}	urea-anion	URE-CL
g_{+E}	cation-ethylene glycol	CHL-ETG
g_{E-}	ethylene glycol-anion	ETG-CL
g_{UU}	urea-urea	URE-URE
g_{EE}	ethylene glycol-ethylene glycol	ETG-ETG

Table 4: Label of the interactions between the compounds

We will used some important features to describe $g_{\alpha\beta}$ and compare them, these features are:

- The position of the main peak.
- The height of the main peak.

We also obtained the MSD of the mixtures using the geometrical center of the molecules as a reference.

In order to make the MSD analysis, we take the central carbon in the choline and urea molecules.

For Etg we take the two central carbons and compare their MSD, finding that they are almost equal, so we use one of the carbons as geometrical center.

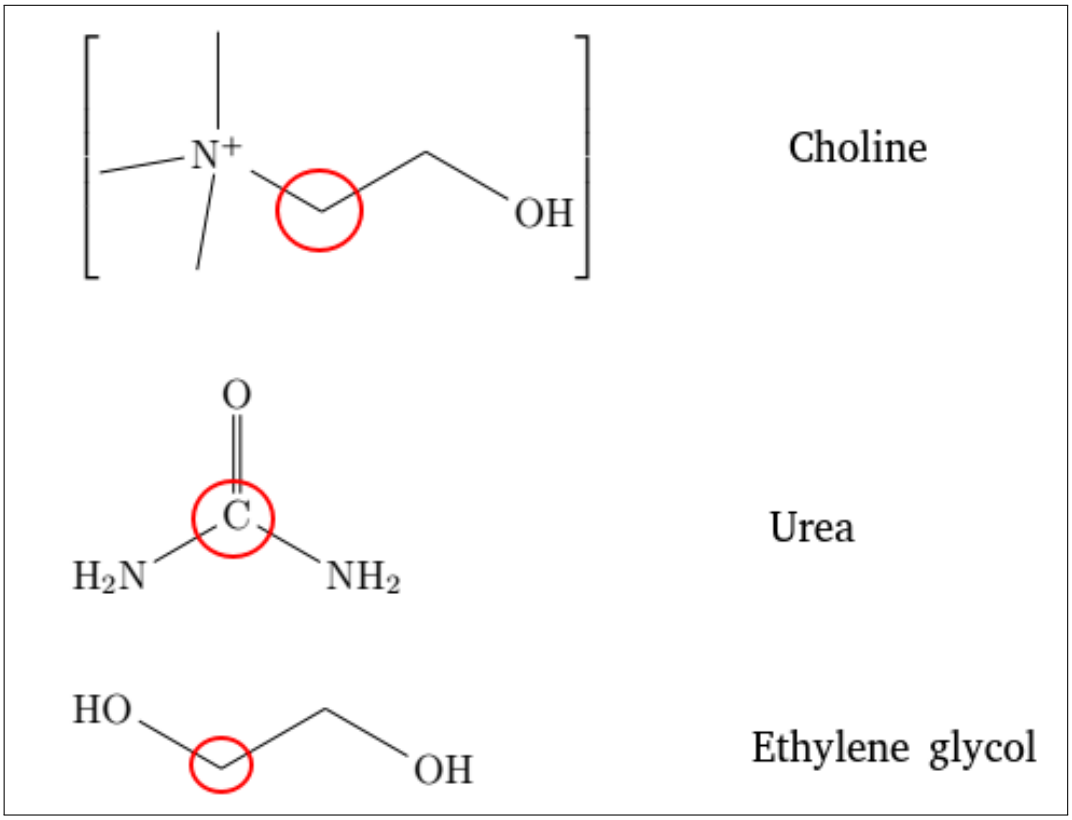

Figure 7: Geometrical center of molecules

From the MSD we calculated the corresponding diffusion coefficient D of

each molecule. Let us now show the comparison of the physical properties described above between the IL versus the Urea DES. Then we compare the IL with the Ethylene glycol DES and finally we compare among the two DES.

4.1 IL vs DES

First we analyzed the RDF and MSD of the IL (ChCl) and then compare them with the DES (ChCl-Ure and ChCl-Etg).

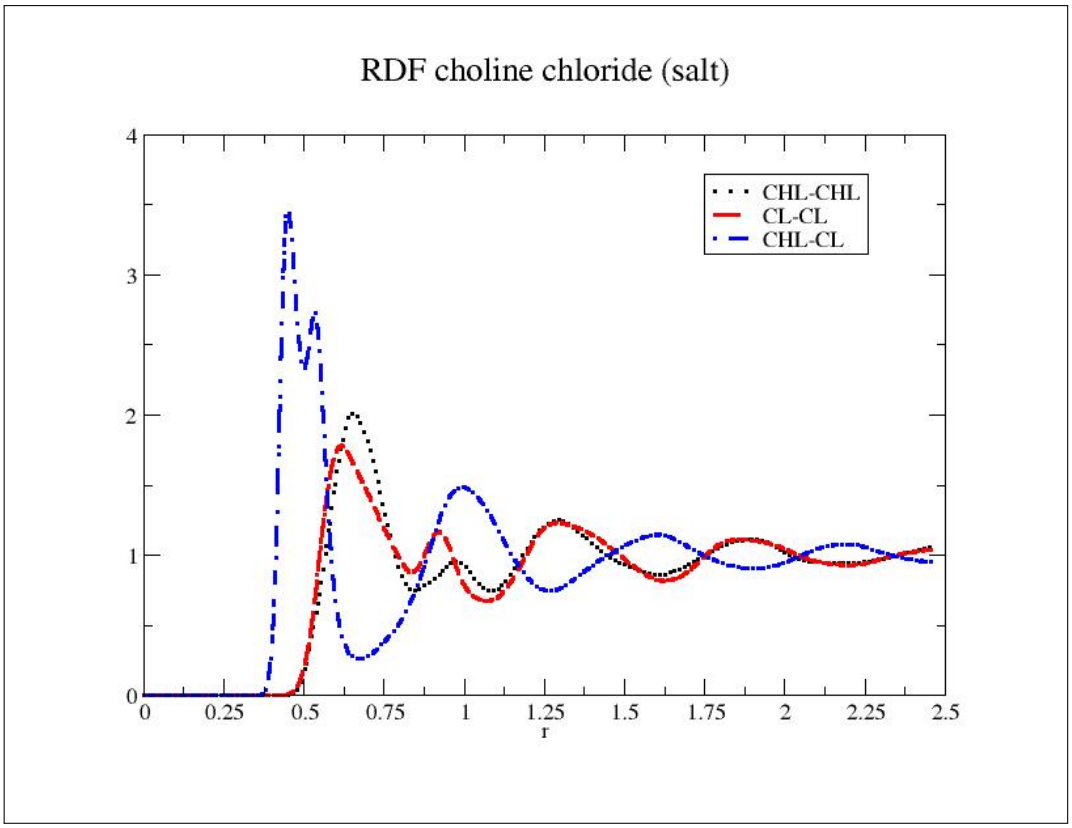

Figure 8: RDF choline chloride

The Fig. 8 shows our calculation of the Radial Distribution Function (RDF) of the IL solvent. The points correspond to the $g_{++}(r)$, the dotted

line to the $g_{--}(r)$ and the point dotted line to the $g_{+-}(r)$. A shift of the main-peak position to larger values is observed for g_{--} and g_{++} compared with g_{+-}.

Notice that the first and second main peaks of g_{+-} are $\approx 0.5nm$. While the first peak of g_{++} and g_{--} is at $\approx 0.625nm$.
The positions of the main peaks of RDF give us information about the strength of the electrostatic interaction among the ions.
We observed that the position of the main peak of g_{+-} is approximately the semi-sum of the effective diameters of the ions (see Table 3). What it does mean is that the electrostatic interactions promote the pairing of the ions.
On the other hand we observe that the mean distance of ions with the same charge are slightly larger for the diameter of the cations (choline), but greater than the effective diameter of the anions.
The separation distance between cations results from a low strength of the repulsive interaction among them. In contrast, the repulsion of the anions is very high as is demonstrated by the great distance between them.
The low repulsion between cations can be understood by the fact that the large size of the cations redistribute the charge in a large area. The huge repulsion among anions is because of the small size of the anions avoids the possibility of a good screening of the anions. As a consequence, the long range repulsion of the anions promotes larger separation distances.

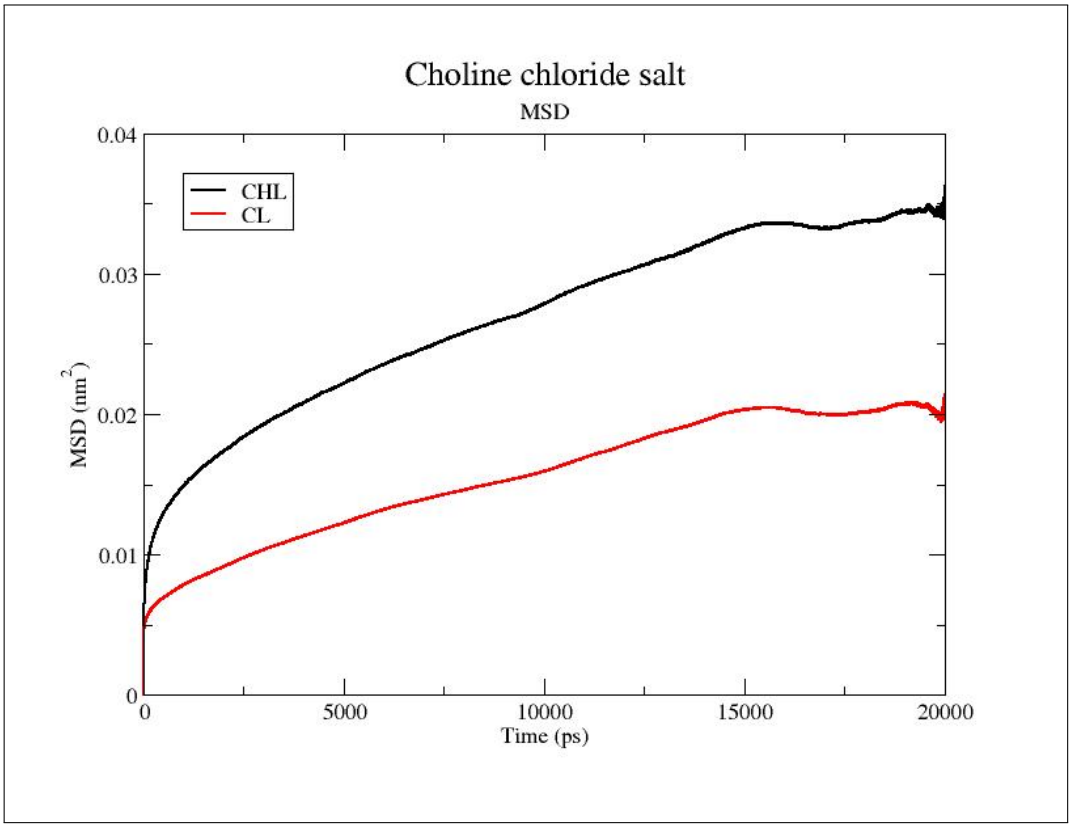

Figure 9: MSD ChCl salt

The Fig. 9 shows the mean-square displacement (MSD) of the IL studied. The black and red line correspond to the cation and anion MSD respectively. An interesting observation can be made, the MSD of the cations are greater that the anions. Such behavior could be quite counter-intuitive because the large particle has a fast mobility. However, is consistent with the usual behavior of IL [23].

4.1.1 IL vs DES (ChCl-Ure)

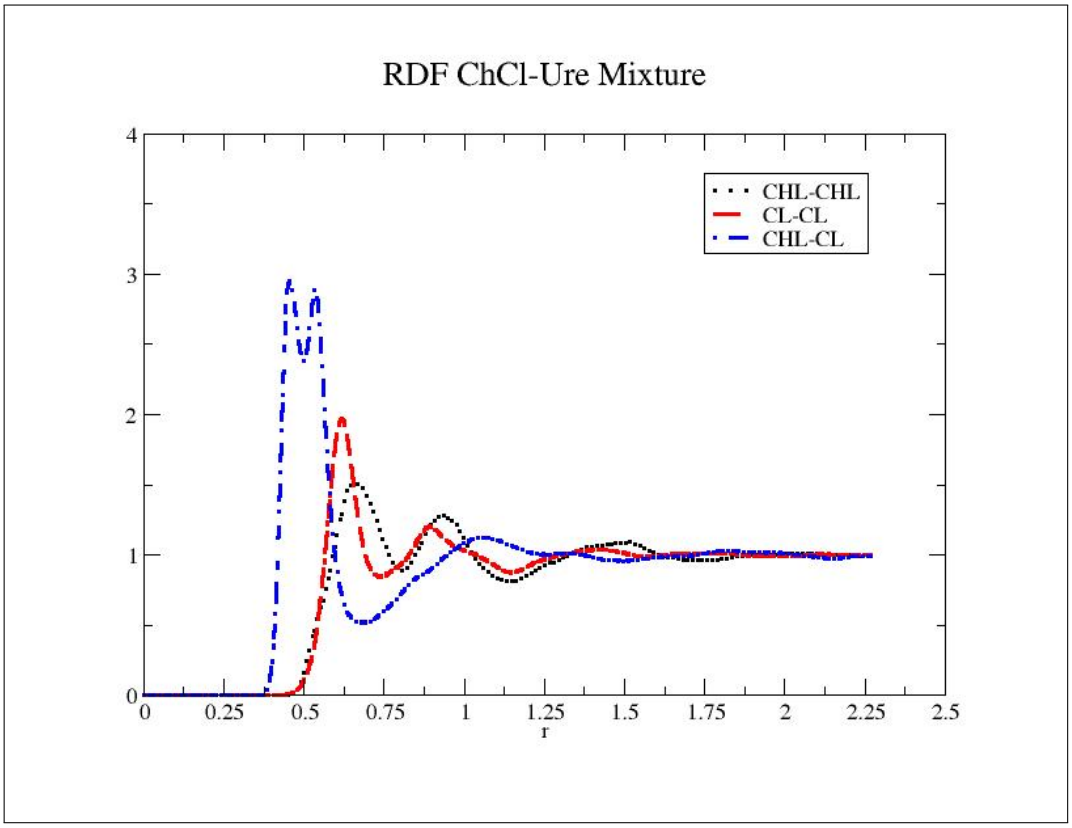

Figure 10: RDF ChCl-Ure Mixture

The Fig. 10 shows our calculation of the RDF of the DES (urea) solvent. The points correspond to the $g_{++}(r)$, the dotted line to the $g_{--}(r)$ and the point dotted line to the $g_{+-}(r)$. A shift of the main-peak position to larger values is observed for g_{--} and g_{++} compared with g_{+-}.

Notice that the first and second main peaks of g_{+-} are $\approx 0.5nm$. While the first peak of g_{++} and g_{--} is at $\approx 0.625nm$.
Like in the IL (ChCl salt) the positions of the main peaks of RDF give us information about the strength of the electrostatic interaction among the ion .
We observed that the position of the main peak of g_{++} is approximately the semi-sum of the effective diameters of the ions (see Table). What it does mean is that the electrostatic interactions promote the pairing of the ions.
The physical aspects of the DES (ChCl-Ure) are the same that the IL but with some differences.
First we can notice that the g_{+-} and g_{++} peaks are shorter and less structured, comparing them with the IL, but the g_{--} remains the same comparing with the IL.

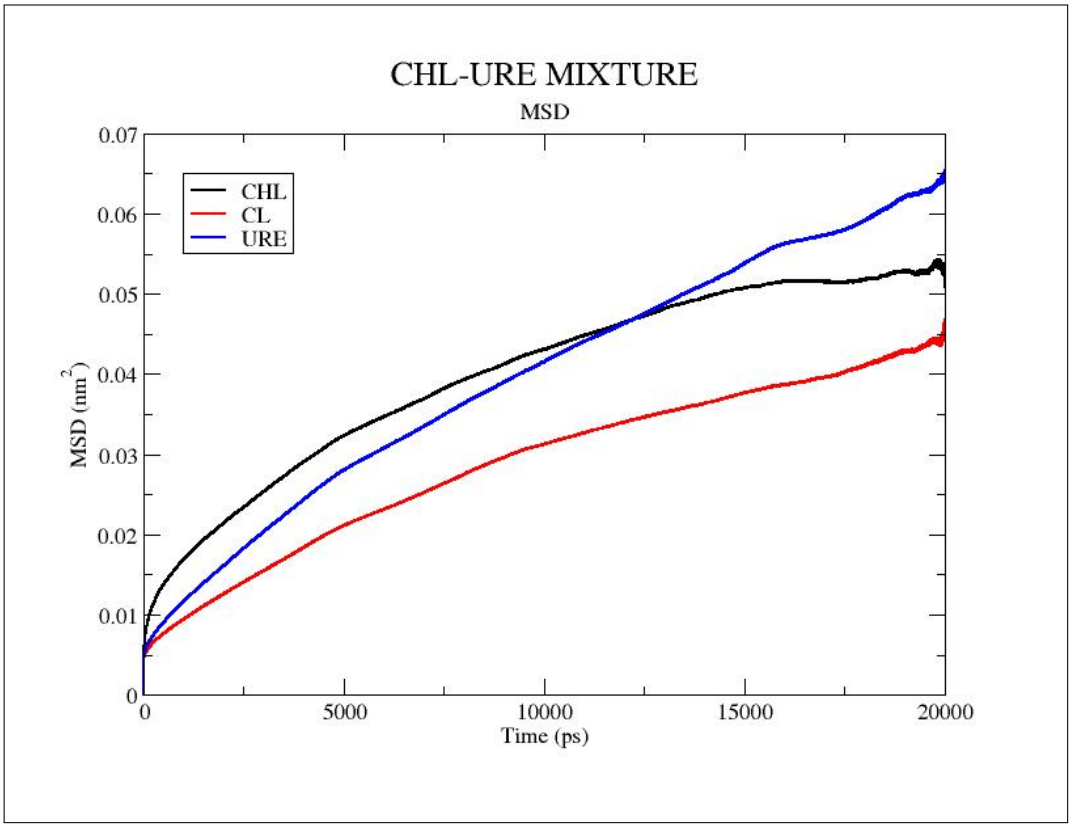

Figure 11: MSD ChCl-Ure

The Fig. 11 shows the MSD of the DES (ChCl-Ure). The black, red, and blue lines, correspond to the cation,anion and urea MSD respectively. The MSD of the cations are greater that the anions like in the MSD of the IL. The MSD of urea is the greater of the three, exhibiting that is the most fluent molecule in the compound.

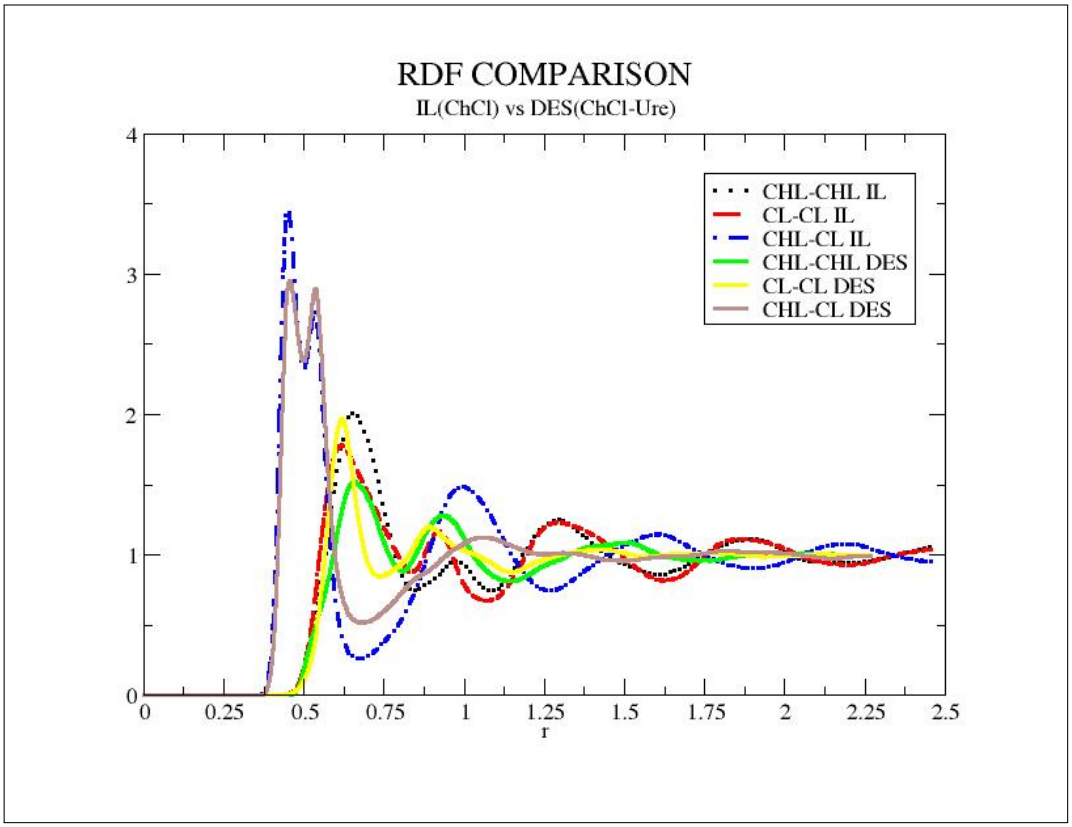

Figure 12: RDF comparison IL vs DES

Fig. 12 Show us the comparison between the IL with the DES (urea), dotted lines, points and point dotted lines correspond to IL and continued lines to DES.
If we compare the g_{+-} of the IL(Blue point dotted line) with the g_{+-} of the DES(Brown line), a notable decrease in the height of the g_{+-} DES is noticed.
Comparing the g_{++} of the IL(Black points) with the g_{++} of the DES(Green line), we can notice a diminishing in the height of the g_{++} of the DES main peak and a little increase in the second peak.
Making a comparison of the g_{--} of the IL(Red dotted line) with the g_{--} of the DES(Yellow line), we can observe a slightly increase in the height of the g_{--} of the DES, but are almost equal.
In the g_{+-}, g_{++} and g_{--}, the main and second peaks remain at the same

distance.
We can notice the effect of the Urea acting like a polarizable solvent, reducing the cation-cation interaction and the cation-anion interaction, but does not affect the anion-anion interaction which is much stronger.

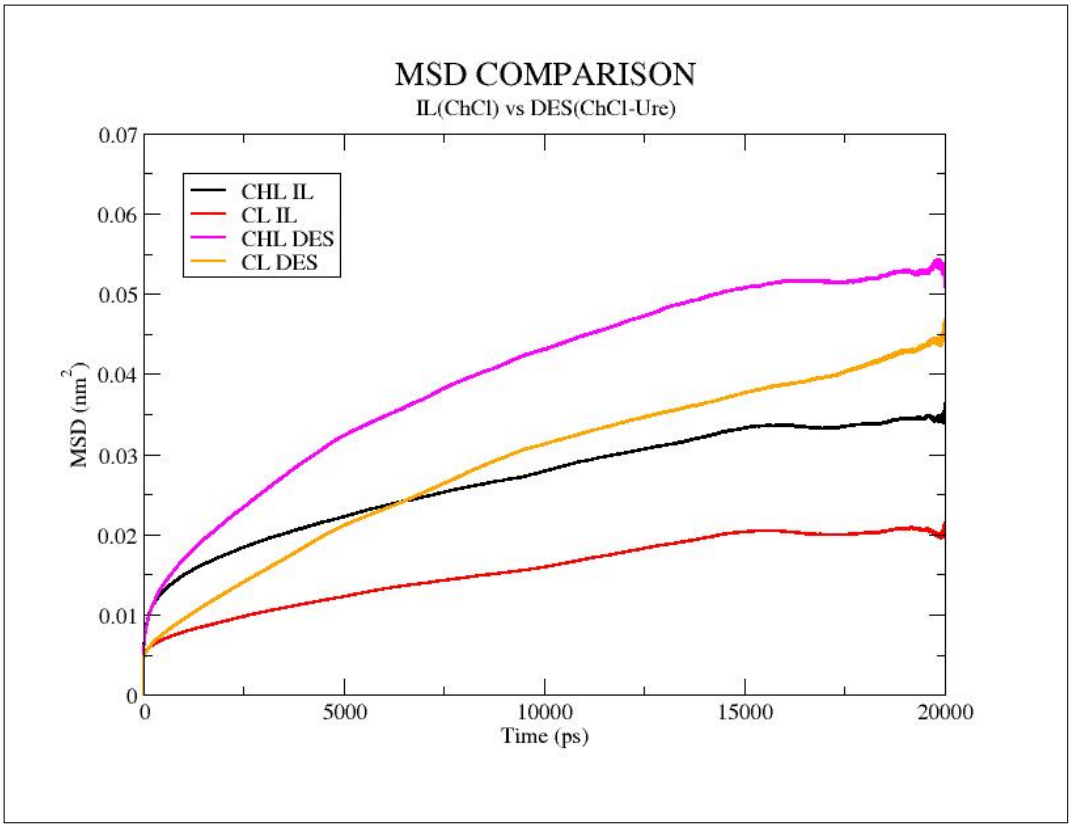

Figure 13: MSD comparison IL vs DES

The Fig. 13 Shows the comparison between the MSD of the DES and the IL. The purple and gold lines correspond to the MSD of the cation and anion in the DES respectively. The black and red lines correspond to the MSD of the cation and anion in the IL respectively. An interesting observation can be made, the MSD of the cations are greater that the anions in both IL and DES but the MSD of the cation and anion of DES are greater than the cation and anion of the IL respectively.

4.1.2 IL vs DES (ChCl-Etg)

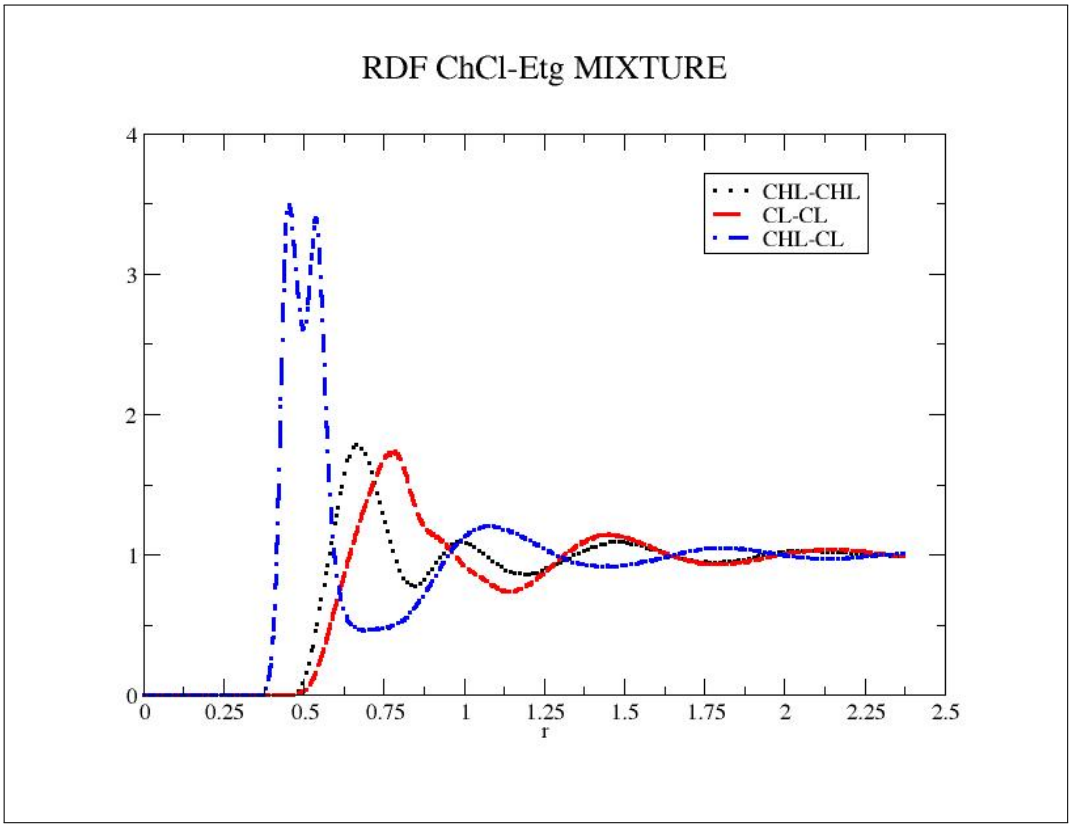

Figure 14: RDF ChCl-Etg Mixture

The Fig. 14 shows our RDF calculation of the DES (Etg). The points correspond to the $g_{++}(r)$, the dotted line to the $g_{--}(r)$ and the point dotted line to the $g_{+-}(r)$. A shift of the main-peak position to larger values is observed for g_{--} and g_{++} compared with g_{+-}, like in the ChCl-urea

mixture.

Notice that the first and second main peaks of g_{+-} are $\approx 0.5nm$. While the first peak of g_{++} is at $\approx 0.625nm$ and the main peak of g_{--} is at $\approx 0.725nm$.
Like in the IL the positions of the main peaks of RDF give us information about the strength of the electrostatic interaction among the ions.
In this DES the distance of the g_{--} is greater than the g_{+-} and g_{++}, making bigger holes were the Etg molecule can diffuse better.
The huge repulsion among anions is because of the small size of the anions avoids the possibility of a good screening of the anions. As a consequence, the long range repulsion of the anions promotes larger separation distances, in this case even greater than the DES (urea) and the IL.

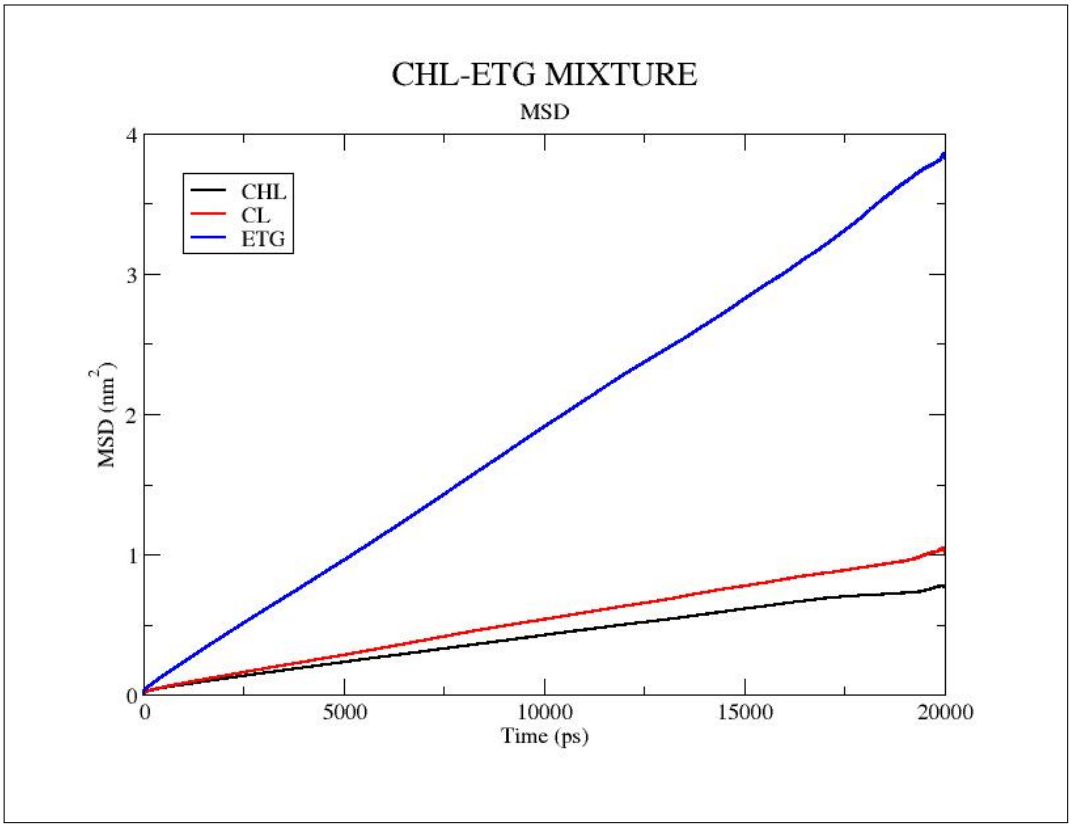

Figure 15: MSD ChCl-Etg

The Fig. 15 shows the MSD of the DES (ChCl-Etg). The black, red, and blue lines, correspond to the cation, anion and Etg MSD respectively. The MSD of the anions are greater that the cations. Such behavior is contrary to the DES (urea) and the IL, were the MSD of the cation is greater than the anion. The MSD of Etg is the greater of the three, exhibiting that is the most fluent molecule in the compound, is more fluid even that the urea if we compare them.

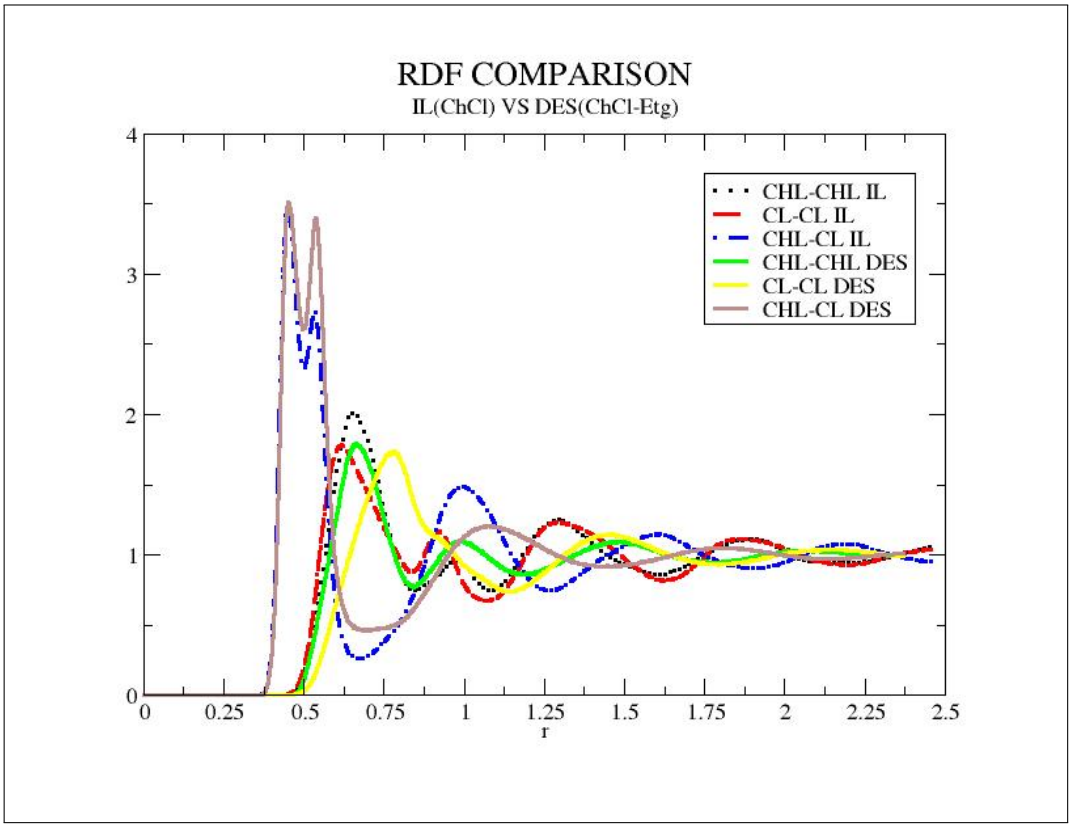

Figure 16: RDF comparison IL vs DES

Fig. 16 Show us the comparison between the IL with the DES (urea), dotted lines, points, and point dotted lines correspond to IL and continued lines to DES.
If we compare the g_{+-} of the IL(Blue point dotted line) with the g_{+-} of the DES(Brown line), a notable increase in the height of the g_{+-} of the DES second main peak and a little decrease of the g_{+-} of the DES second peak are noticed.
Comparing the g_{++} of the IL(Black points) with the g_{++} of the DES(Green line), we can notice a little diminishing in the height of the g_{++} of the DES main peak.
Making a comparison of the g_{--} of the IL(Red dotted line) with the g_{--} of the DES(Yellow line), we can observe a difference in the distance main peak of the g_{--} of the DES, but the height is equal.

In the g_{+-} and g_{++}, the main and second peaks remain at the same distance.
We can notice the effect of the Etg acting like a solvent, reducing the cation-cation interaction and the cation-anion interaction, but principally affecting the anion-anion interaction increasing the distance between the anions and creating holes where the Etg molecule can diffuse better.

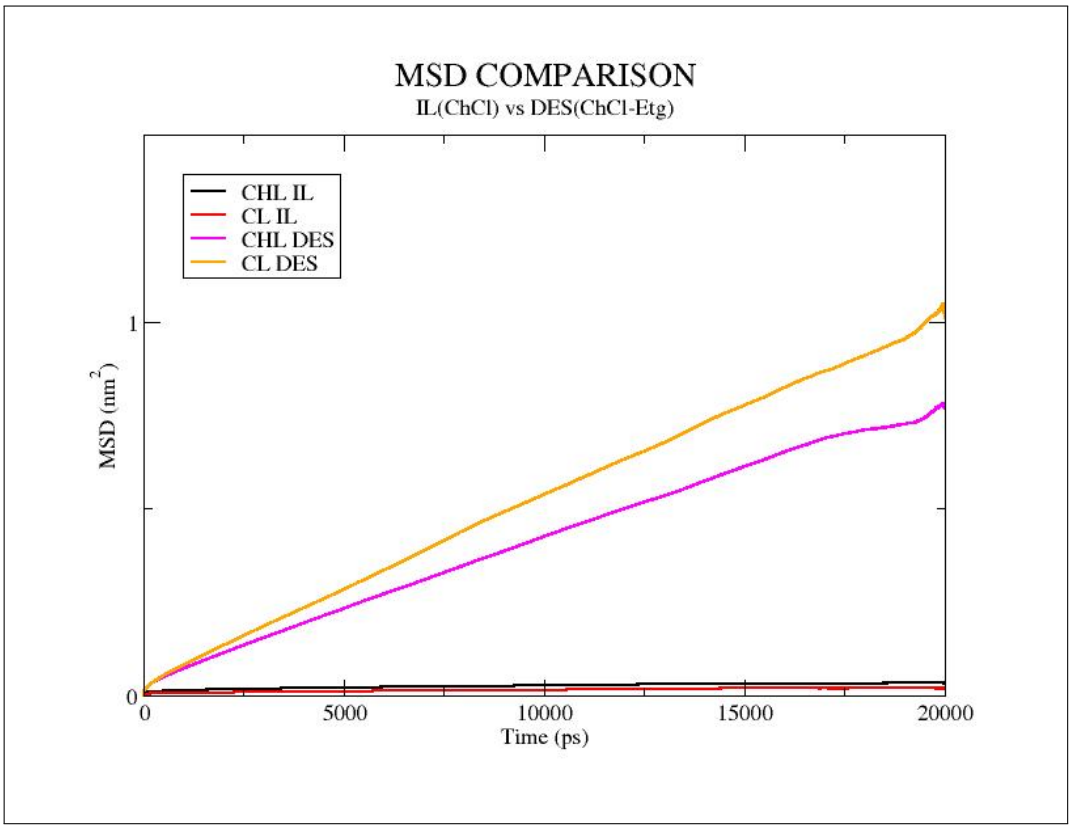

Figure 17: MSD comparison IL vs DES

The Fig. 17 Shows the comparison between the MSD of the DES and the IL. The purple and gold lines correspond to the MSD of the cation and anion in the DES respectively. The black and red lines correspond to the MSD of the cation and anion in the IL respectively. The MSD of the anions in the case of the DES is greater that the cations, showing the mobility

caused by the holes created by the Etg molecule in the DES. This is a notorious difference compared with the IL and DES(urea) in which the cations were more fluid than the anions.

4.2 DES(ChCl-Ure) vs DES(ChCl-Etg)

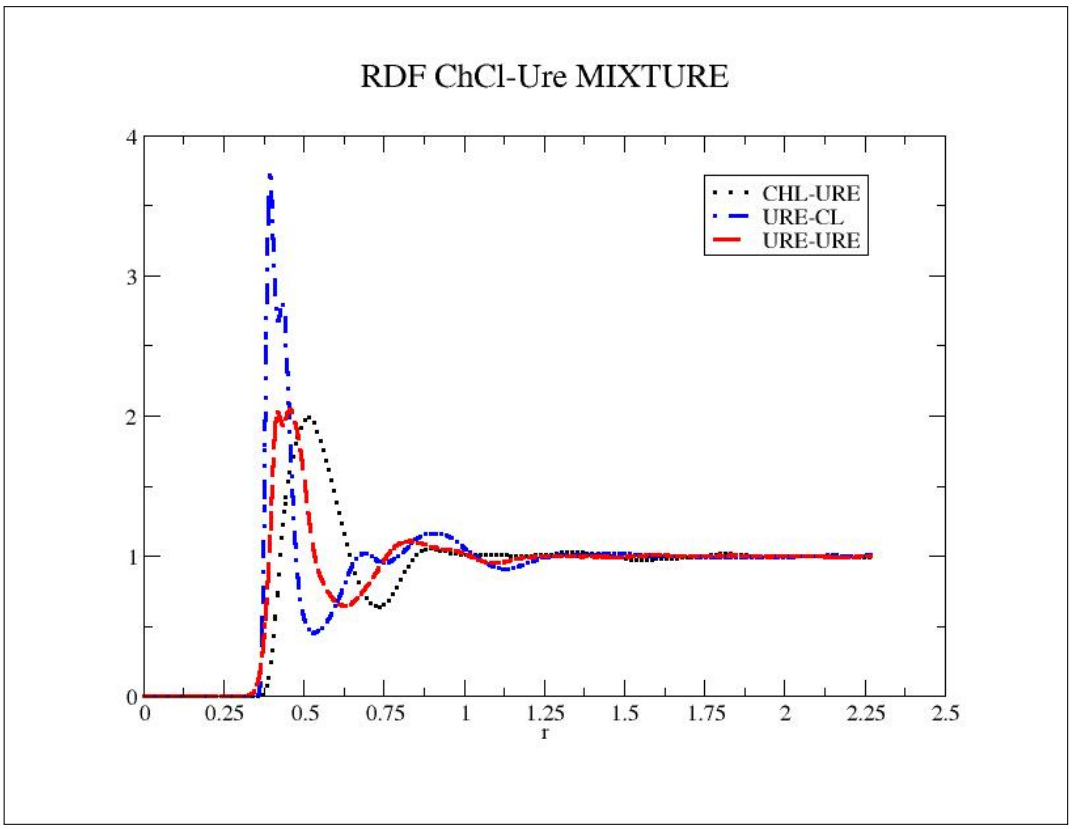

Figure 18: RDF ChCl-Ure Mixture

The Fig. 18 shows our calculation of the RDF of the DES (urea) solvent. The points correspond to the $g_{+U}(r)$, the point dotted line to the $g_{U-}(r)$ and the dotted line to the $g_{UU}(r)$.

In this plot we do not observe a phase shifting, but we can see that the urea molecule acted like a cation when interacts with the choline and chloride molecules, and like a Lennard Jones liquid when interacts with itself.
The g_{U-} main peak is at $\approx 0.375\ nm$ that is the semi-sum of the urea atomic diameter and the chloride ionic diameter,that implies an attractive interaction between the molecules.
The g_{U+} main peak is at $\approx 0.50\ nm$ that is more than the the semi-sum of the urea atomic diameter and the choline ionic diameter, like a repulsive interaction between molecules.
The g_{UU} main peak is at $\approx 0.380\ nm$ that is the approximate urea atomic diameter, so there is not an electrostatic interaction among the molecules, or if there is an electrostatic interaction it must be very week.

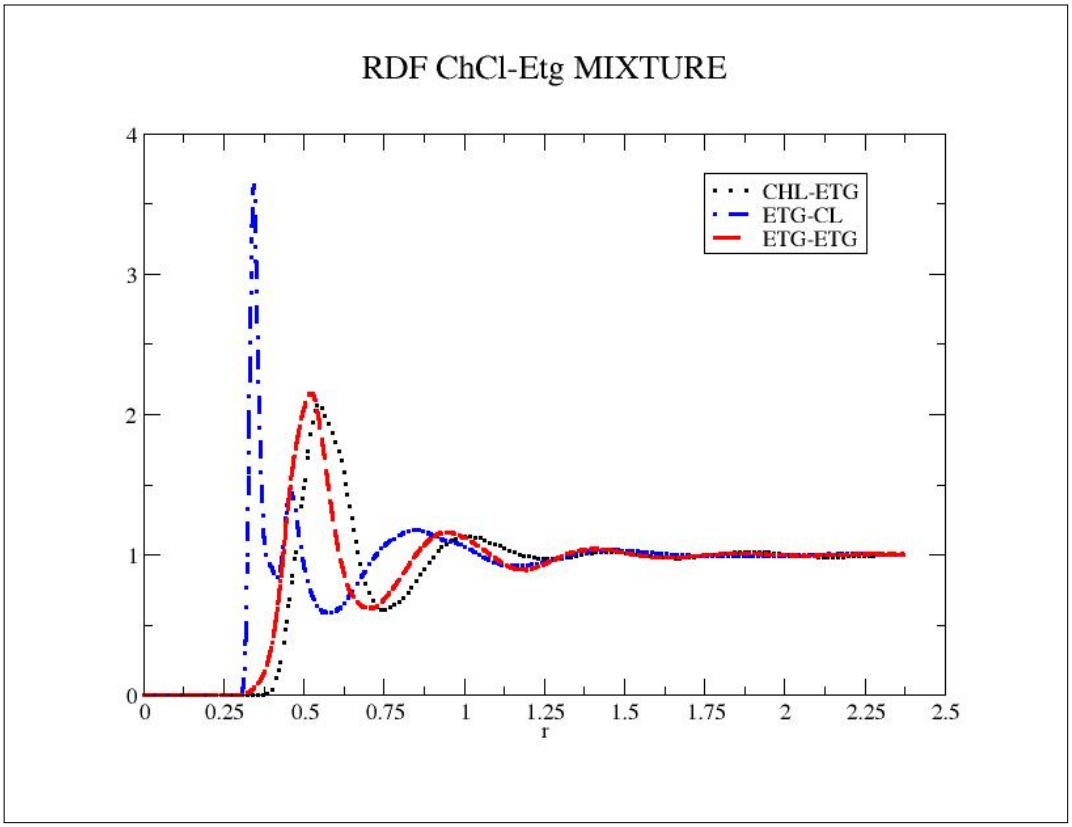

Figure 19: RDF ChCl-Etg Mixture

The Fig. 19 shows our calculation of the RDF of the DES (Etg) solvent. The points correspond to the $g_{+E}(r)$, the point dotted line to the $g_{E-}(r)$ and the dotted line to the $g_{EE}(r)$.

In this picture we do not observe a phase shifting, but we can see that the Etg molecule acted also like a cation when interacts with the choline and chloride molecules, and like a Lennard Jones liquid when interacts with itself.
The g_{U-} main peak is at $\approx 0.375\ nm$ that is the semi-sum of the Etg atomic diameter and the chloride ionic diameter,that implies an attractive interaction between the molecules.
The g_{U+} main peak is at little bit more than $\approx 0.50\ nm$ that is more than the the semi-sum of the Etg atomic diameter and the choline ionic

diameter, like a repulsive interaction between molecules.
The g_{EE} main peak is at $\approx 0.50\ nm$ that is little more than the approximate Etg atomic diameter, so there is a week electrostatic interaction among the molecules, that made the molecules to be acting like cations among them.

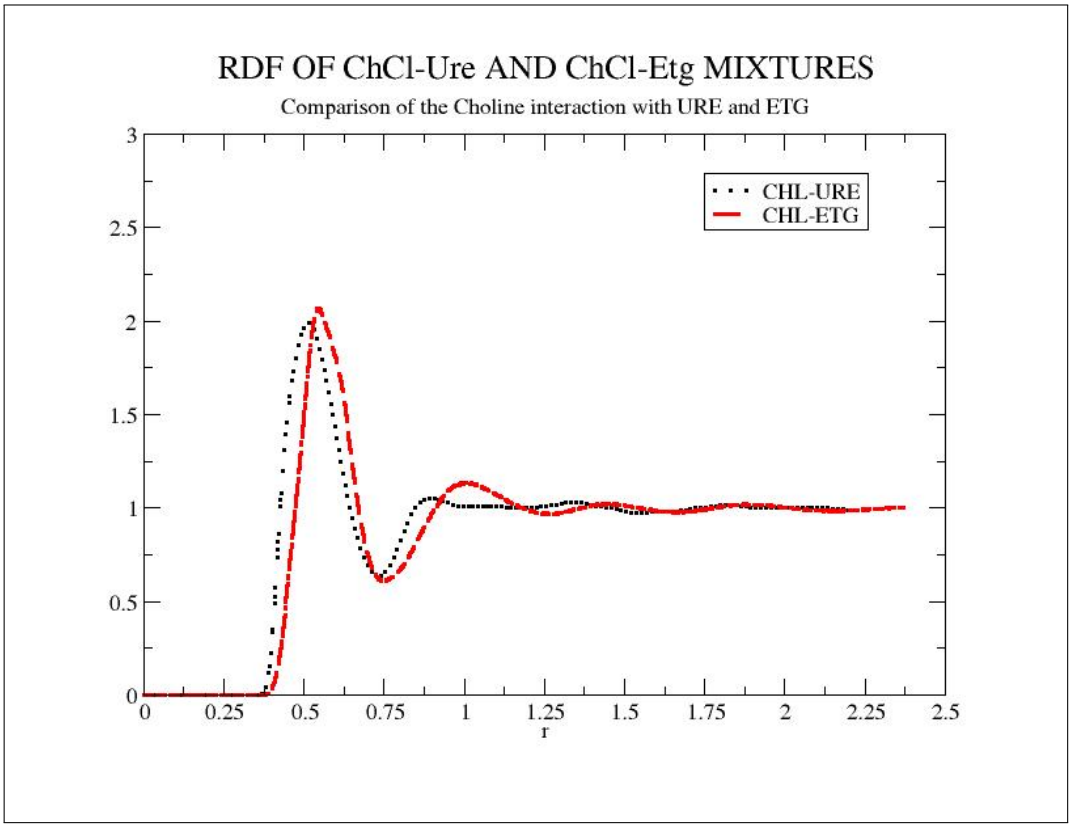

Figure 20: RDF ChCl-Ure and ChCl-Etg Mixtures with the cation

The Fig. 20 shows our calculation of the RDF of the DES (urea and Etg) interacting with the cation (choline) in the mixtures. The points correspond to the $g_{+U}(r)$ and the dotted line to the $g_{+E}(r)$.
In this plot we noticed that the main peak of the g_{+u} and g_{+E} are greater than the semi-sum of their molecular diameters and the choline ionic diameter, indicating that there is a repulsive interaction between the urea and Etg with choline.
Therefore the urea and Etg act like cations when interact with choline molecules.
The main peaks of g_{+U} and g_{+E} are at $\approx 0.5\ nm$.
The g_{+U} and g_{+E} of systems are almost equal and both showed very poor structure on the second peak.

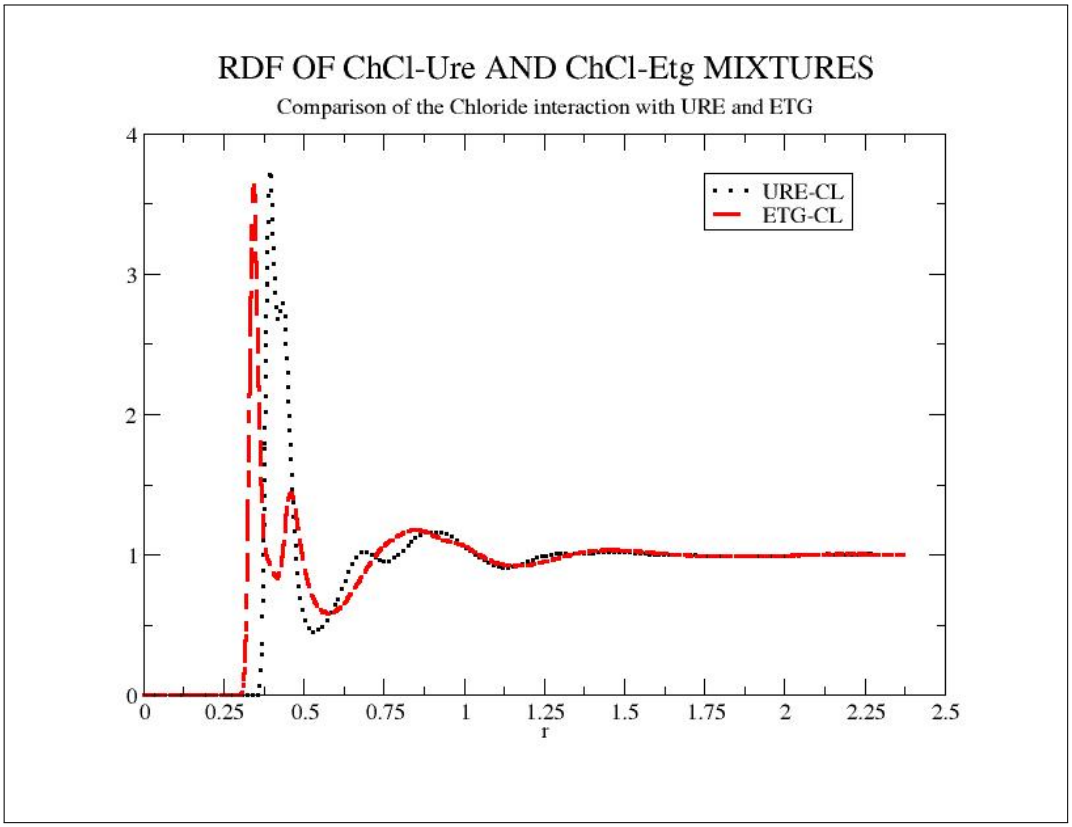

Figure 21: RDF ChCl-Ure and ChCl-Etg Mixtures with the anion

The Fig. 21 shows our calculation of the RDF of the DES (urea and Etg) interacting with the anion (chloride) in the mixtures. The points correspond to the $g_{U-}(r)$ and the dotted line to the $g_{E-}(r)$.
In this plot we noticed that the main peak of the g_{+u} and g_{+E} are approximate than the semi-sum of their molecular diameters and the chloride ionic diameter, indicating that there is an attractive interaction between the urea and Etg with chloride.
We can observe that g_{U-} and g_{E-} have almost the same main peak height, except for a little bump at $\approx 0.5\ nm$, both systems show very similar structure.
The distance of g_{U-} is $\approx 0.375\ nm$ and the distance of g_{E-} is a little less than $\approx 0.375\ nm$.

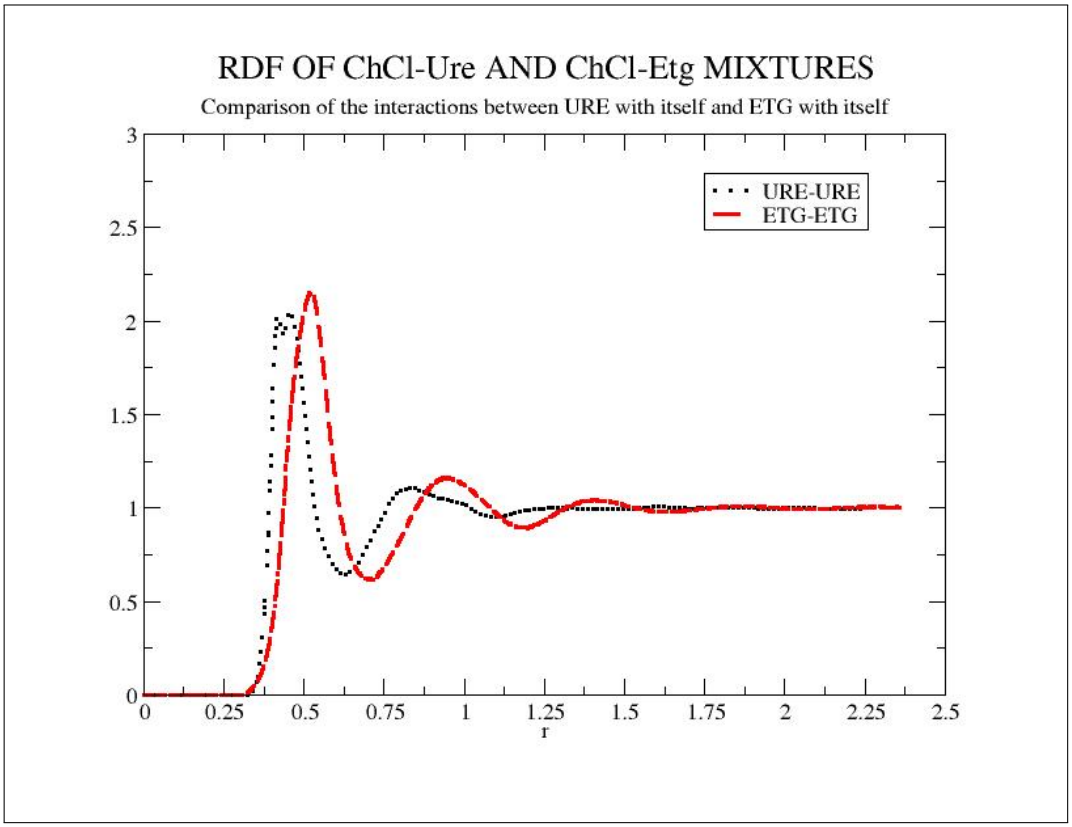

Figure 22: RDF ChCl-Ure and ChCl-Etg Mixtures with them-self

The Fig. 22 shows our calculation of the RDF of the DES (urea and Etg) interacting with themselves in the mixtures. The points correspond to the $g_{UU}(r)$ and the dotted line to the $g_{EE}(r)$.
In this picture we noticed that the main peak of the g_{+u} is similar to the molecular diameter of urea, therefore, urea molecules interact like a Lennard-Jones liquid with itself, but g_{+E} is greater than the approximate molecular diameter of Etg, indicating that there is a little repulsive interaction between the Etg and itself.
We can observe that g_{UU} and g_{EE} has almost the same hight, but g_{UU} is a little bit taller.
In addition g_{EE} is more structured than g_{UU}.

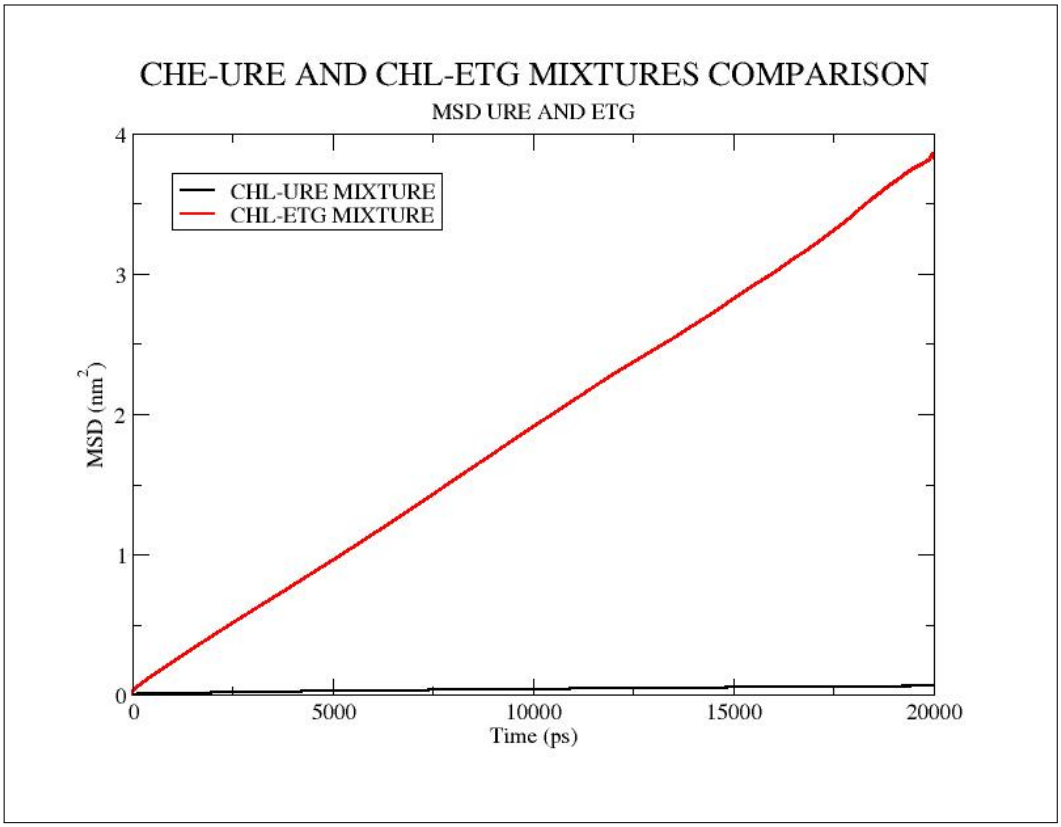

Figure 23: MSD *Ure* vs *Etg*

The Fig. 23 shows the MSD of the DES(ure) vs DES(Etg). The black and red line correspond to the urea MSD and Etg MSD respectively. An interesting observation can be made, the MSD of Etg is greater that the urea, showing that Etg molecules diffuse more that the urea molecules.

4.3 Comparison of the cation and anion interactions

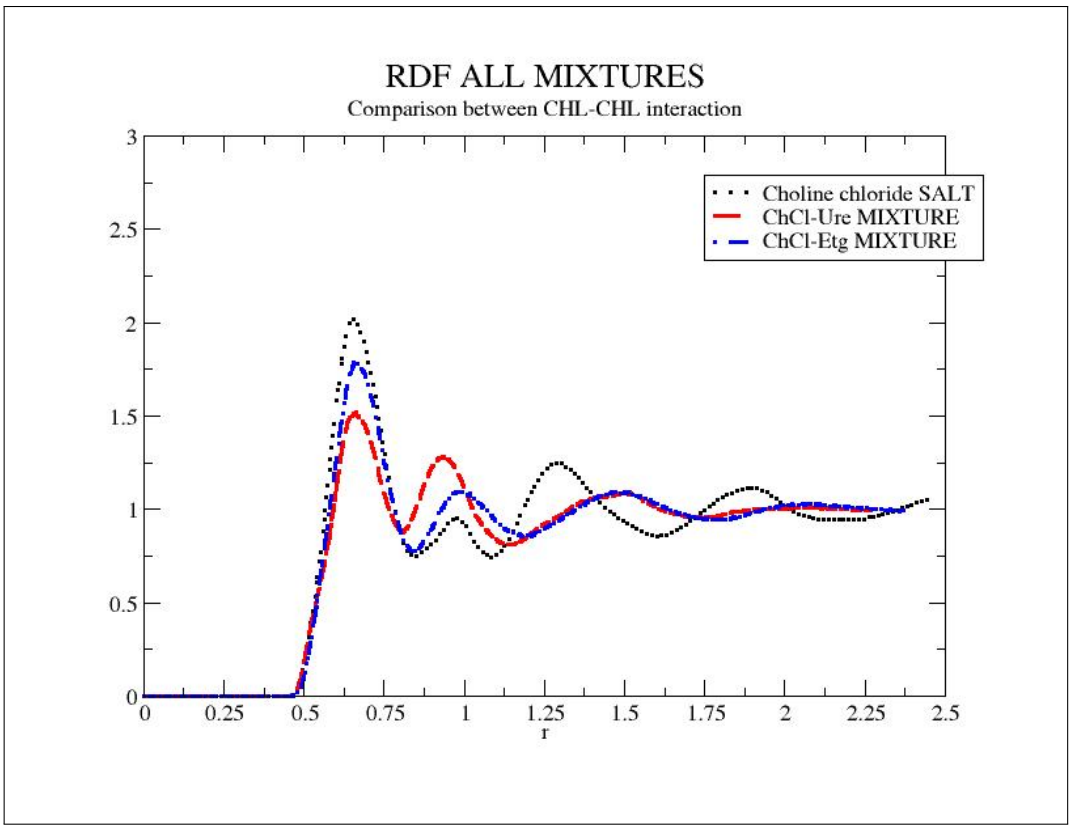

Figure 24: RDF all Mixtures (cation-cation interaction)

The Fig. 24 shows our calculation of the RDF for the choline-choline (cation-cation) interactions of the IL and the two DES. The points correspond to the IL, the dotted line to the DES(urea) and the point dotted line to the DES(Etg).

In this plot we can observe that the g_{++} interactions in the three systems has the same distance to the first peak $\approx 0.625\ nm$, that is, the repulsive interaction between the cations in the system.
The g_{++} in the ChCl salt has a higher main peak and has a greater structure, followed by the ChCl-Etg mixtures and at last the ChCl-Ure mixture.
The g_{++}'s are very similar, despite the height of main and second peaks.

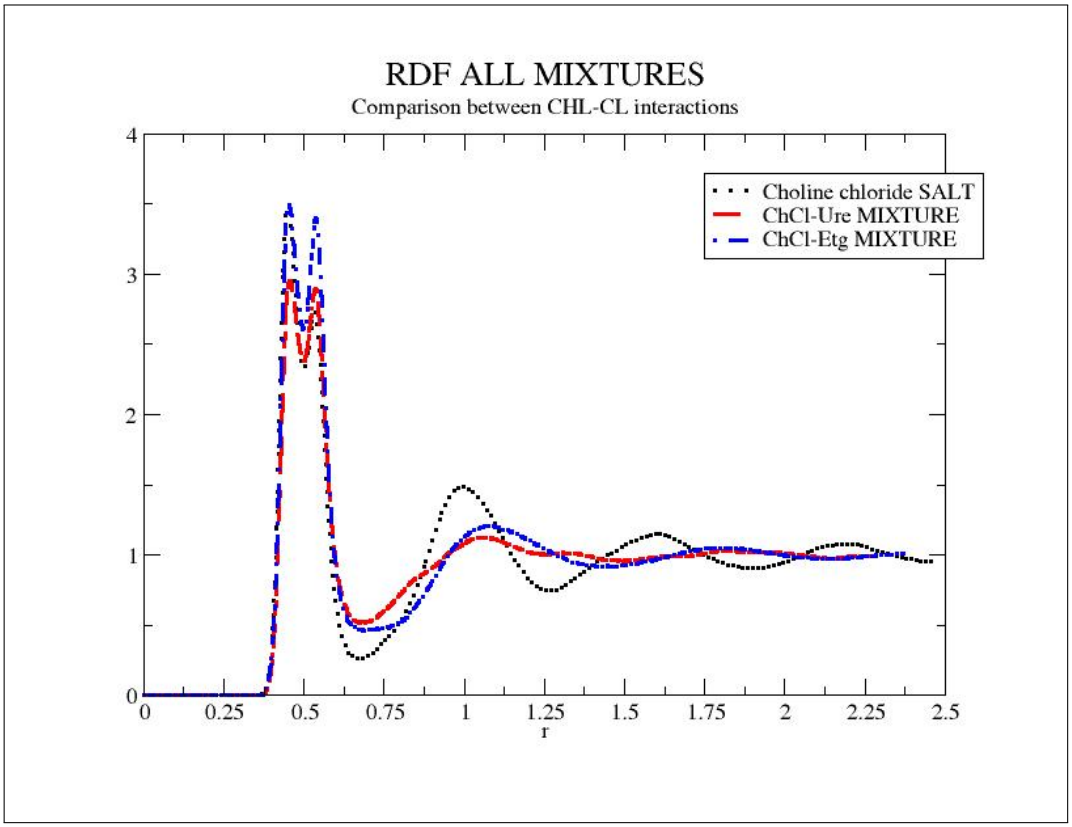

Figure 25: RDF all Mixtures (cation-anion interaction)

The Fig. 25 shows our calculation of the RDF for the choline-chloride (cation-anion) interactions of the IL and the two DES. The points correspond to the IL, the dotted line to the DES(urea) and the point dotted line to the DES(Etg).

In this plot we observe that the two main peaks are at the same distance distance in the three systems.
The distance of the first main peak is $\approx 0.45\ nm$, and the distance of the second main peak is $\approx 0.54\ nm$. The g_{+-} in the ChCl salt and ChCl-Etg, has the same height in the first main peak, but ChCl-Etg mixture has a taller second main peak, nevertheless ChCl salt shows a greater structure. The g_{+-} in the ChCl-Ure mixture showed the shortest peaks and less structure of the systems.

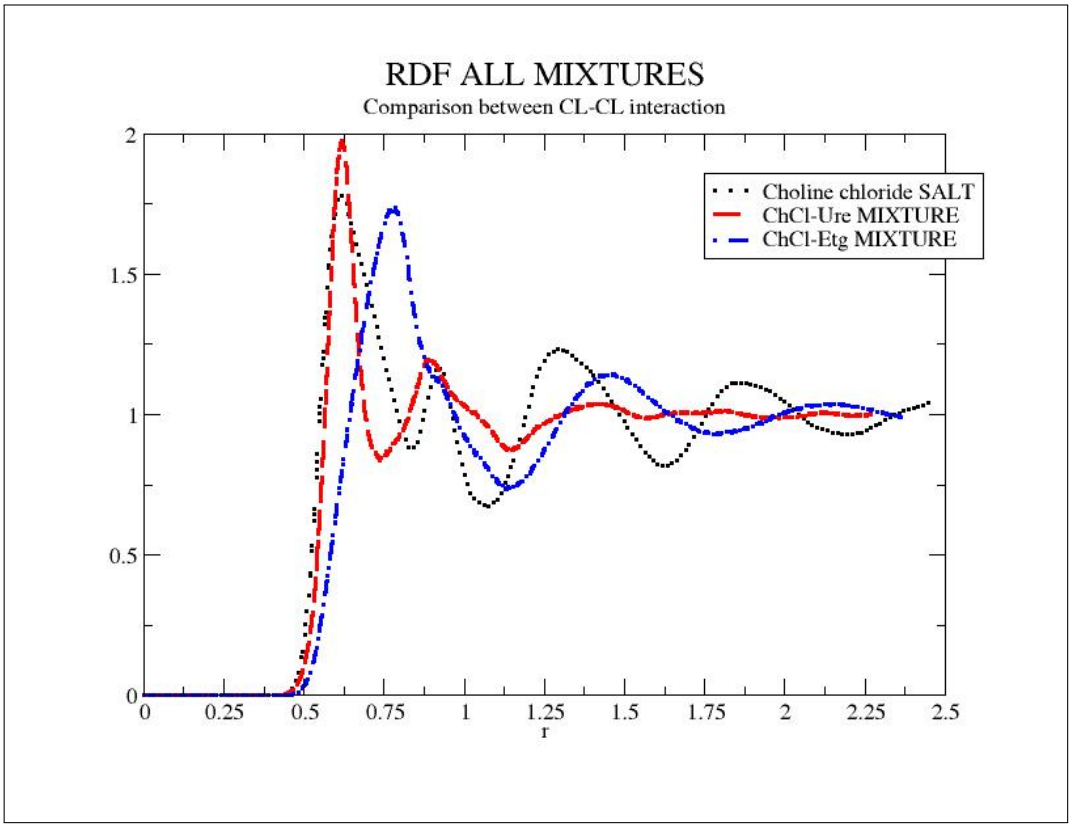

Figure 26: RDF all Mixtures (anion-anion interaction)

The Fig. 25 shows our calculation of the RDF for the choline-chloride (anion-anion) interactions of the IL and the two DES. The points correspond to the IL, the dotted line to the DES(urea) and the point dotted line to the DES(Etg).

In this plot we can observe that the main peak distance of g_{--} is the same $\approx 0.625\ nm$ in the ChCl salt and ChCl-Ure systems, but the main peak distance of g_{--} in the ChCl-Etg mixture is $\approx 0.75\ nm$.

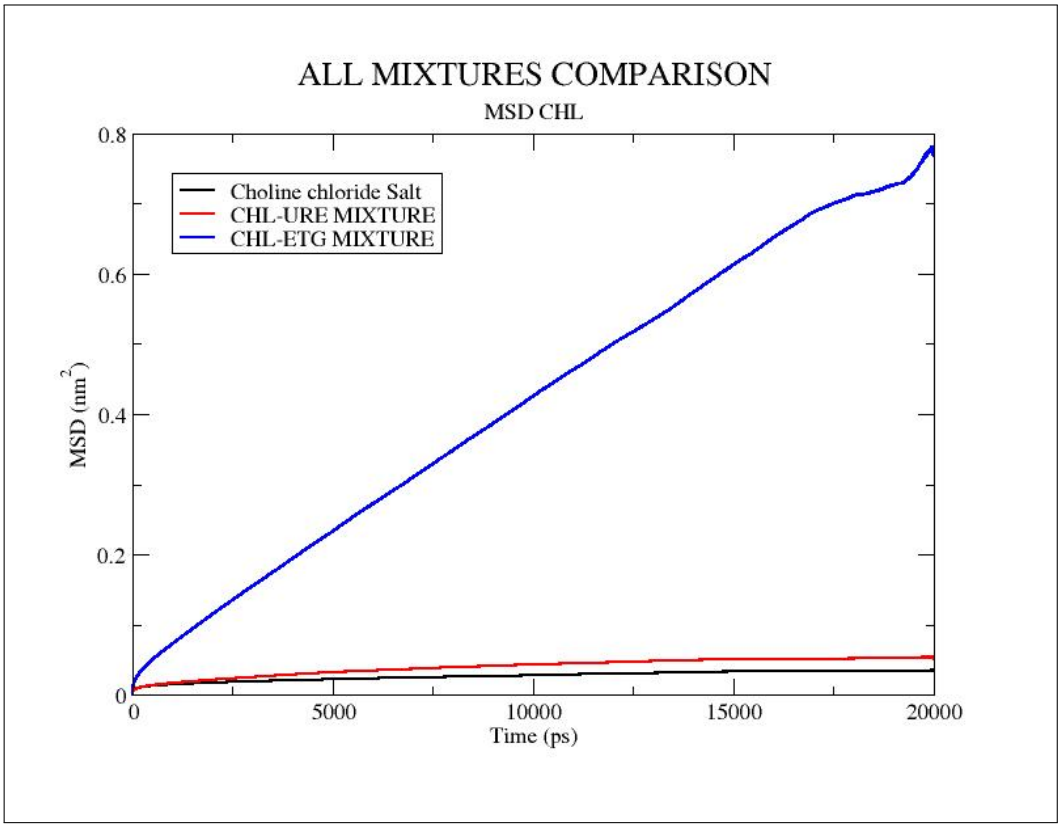

Figure 27: MSD of Choline in all mixtures

The Fig 27. clearly shows us the huge difference of the diffusion in the DES (Etg) compared with IL and the DES (Urea).

4.4 Summary

In this section we present an overall picture of the principal observations reviewed in the previous sections. We have focused in the principal features extracted from our analysis of the radial distribution functions. The aim of this section is the obtaining of general physical insights about the molecular differences among the studied solvents.

In order to obtain a qualitative idea about the strength of the molecular interactions we observe the position and the height of the main peak of RDF. It is well known that those data are related with the mean distance of first neighbors and the coordination number. Hence, low values of the position of the main peak means a strong attraction of the molecules. While, large values of the height mean peak are related with a locally crowded system. With the aim of evaluate such kind of qualitative properties we propose a the method described by the following table:

Structure of the RDF	Meaning
Very	A very structure $g(r)$ is represented by a high and thin main peak, with a definite gap between the main and second peak, that represent a solid-like structure
Normal	A normal structure $g(r)$ is represented by a not so high main peak(2 or less than 3 first neighbors), and the with of the first peak is $\approx 0.5\ nm$, the gap between the main and the second peak is still visible, that represent a liquid-like structure.
Less	A less structure $g(r)$ is represented by a short peak(less than 2 first neighbors) and the with of the main peak is greater than $\approx 0.5\ nm$, there is not a gap or a very little gap between the main and second peak, that represent a gas-like structure

Table 5: Types of Structures of the RDF and their meaning.

Interaction of the ions [+] [−] among the mixtures.

g_{+-}	Distance		Main peak height		Structure
ChCl salt	0.45	0.54	3.5	2.6	Very
ChCl-Ure	0.45	0.54	3.0	3.0	Normal
ChCl-Etg	0.45	0.54	3.5	3.5	Normal

Table 6: Behavior of g_{+-} in different mixtures.

g_{++}	Distance	Main peak height	Structure
ChCl salt	0.625	2.0	Very
ChCl-Ure	0.625	1.50	Less
ChCl-Etg	0.625	1.70	Normal

Table 7: Behavior of g_{++} in different mixtures.

g_{--}	Distance	Main peak height	Structure
ChCl salt	0.625	1.75	Very
ChCl-Ure	0.625	2.0	Less
ChCl-Etg	**0.750**	1.75	Normal

Table 8: Behavior of g_{--} in different mixtures.

Interaction of the ions [+] [−] with Urea and Ethylene glycol.

ChCl-Ure mixture	Distance	Main peak height	Structure
g_{+U}	0.5	2.0	Normal
g_{U-}	0.375	3.75	Very
g_{UU}	0.375	2	Normal

Table 9: Interaction of Urea with the cation, anion and itself in different mixtures.

ChCl-Etg mixture	Distance	Main peak height	Structure
g_{+E}	0.5	2.0	Normal
g_{E-}	0.375	3.75	Very
g_{EE}	0.5	2	Normal

Table 10: Interaction of Etg with the cation, anion and itself in different mixtures.

The Diffusion constants of CHL^+, Cl^-, URE and ETG are compared in the next tables.

The units used in the diffusion constant are $1x10^{-5}$ cm^2/s.

CHL^+	Diffusion constant	$+/-$
ChCl salt	0.0002	0.0001
ChCl-Ure	0.0003	0.0002
ChCl-Etg	0.0063	0.0003

Table 11: MSD comparison of CHL^+ in all the mixtures

Cl^-	Diffusion constant	$+/-$
ChCl salt	0.0001	0.0000
ChCl-Ure	0.0003	0.0002
ChCl-Etg	0.0081	0.0006

Table 12: MSD comparison of Cl^- in all the mixtures

Mixtures	Diffusion constant	$+/-$
ChCl-Ure	0.0004	0.0001
ChCl-Etg	0.0311	0.0002

Table 13: MSD comparison ETG vs URE

After this summary, we generally observed that the height of the main peaks are smaller for the DES compared with the RTMS (Room Temperature Molten Salt).
Besides, the diffusion coefficients of the RTMS are lower than in the DES. From the data presented we can conclude that, at least for the solvents studied, the presence of the third component (Urea or Ethylene glycol) reduces the number of first neighbors, which means that the molecular correlations are weaker than the RTMS. In addition, we observe an increasing of the mobility in the DES. Our observations can be interpreted as an overall reduction of the effective electrostatic interaction of the ions.

5 Thermochemical analysis of IL and DES

In order to obtain a better understanding of the properties of IL an DES, we applied a simple thermodynamical model to estimate the stability of the crystalline phase of the system. The approach has been adapted from the work of Kapustinskii [7] and Born-Mayer [7] [5]. The model calculates the lattice enthalpy which estimates the energy barrier needed for melting the crystalline phase. If such barrier is high then the crystal is hard to melt. Systems with high values of lattice enthalpy usually have a higher melting temperature.

The application of the thermodynamic approach presented below requires the following assumptions :

- The ions are treated as hard spheres.
- The hard spheres are non-polarizable.
- The charge of the ion is concentrated in the center of the sphere.
- In the case of the DES, the Urea and Etg are treated as effective solvents with dielectric constant ϵ.

  We extended this ideas to model the main features in the IL and DES compounds in a solid crystalline structure and in aqueous and non-aqueous solutions.

  Despite its simplicity, this model can exhibit the essential behavior of this complex compounds in a clear and effortless way.

5.1 The Born-Mayer equation

The Born-Mayer equation is a closed expression for the lattice enthalpy of a crystal formed by charged components. Such model has been applied to classical salts as sodium chloride [7]. In order to derive the Born-Mayer equation let us consider a ionic crystal in which the ions are arranged in a regular lattice with a lattice distance d. The system satisfy the electroneutrality condition (the net charge of the system is equal to zero) and the charges of the cations and anions are $+e$ and $-e$ respectively.

To obtain the energy of the system we need to calculate the Coulombic potential of the structure of ions. First we calculate the potential of a single cation, that is the sum of interactions with all the other ions and is given by :

$$V = \frac{2e^2}{4\pi\epsilon_0}\left(-\frac{1}{d} + \frac{1}{2d} - \frac{1}{3d}\right)$$

The sum of the series in parenthesis is equal to $ln\ 2$ therefore we have :

$$V = -\frac{2e^2\ ln\ 2}{4\pi\epsilon_0 d}$$

The factor $ln\ 2$ is an example of a Mandelug constant that represent the geometrical distribution of the ions.

$$V = -\frac{2e^2}{4\pi\epsilon_0 d}A$$

If we multiplied the Avogadro's number to this potential, we obtain the total molar contribution of all the ions to the potential energy, and divided by 2 to avoid counting each interaction twice we have :

$$V = -N_A\frac{e^2}{4\pi\epsilon_0 d}A$$

To obtain the total molar potential energy, a repulsive interaction between the ions is needed.

The function $B\exp\left(-\frac{d}{d^*}\right)$ is used to model the repulsive interaction between the ions, this is a short-range exponential function, where d^* is a constant that defines the range of the repulsive interactions and B is a constant that defines its magnitude.

$$V = -\frac{N_A\ e^2}{4\pi\epsilon_0 d}A + B\exp\left(-\frac{d}{d^*}\right)$$

Deriving with respect the distance and equating to zero the last equation to obtain the minimum of the potential energy :

$$\frac{\mathrm{d}\ V}{\mathrm{d}\ d} = 0$$

$$\frac{N_A\ e^2}{4\pi\epsilon_0 d^2}A - \frac{B}{d^*}\exp\left(-\frac{d}{d^*}\right) = 0$$

At the minimum, the short-rage exponential can be represented as :

$$B\exp\left(-\frac{d}{d^*}\right) = \frac{N_A\ e^2\ d^*}{4\pi\epsilon_0 d^2}A$$

Substituting in the equation for V :

$$V = -\frac{N_A\ e^2}{4\pi\epsilon_0 d}\left(1 - \frac{d^*}{d}\right)A$$

V is the energy to form the lattice from the ions in the gas state, at T=0 we have :

$$\Delta H^\circ = -\Delta U^\circ$$

The change in sign is because we are taking the gas ions to form the lattice, that implies a release in energy

$$M^+(g) + X^-(g) \quad \rightarrow \quad MX(s) \qquad\qquad -\Delta H^\circ$$

Therefore we have that :

$$\Delta H^\circ = \frac{N_A |z_+ z_-| e^2}{4\pi\epsilon_0 d}\left(1 - \frac{d^*}{d}\right) A$$

in which

- $d = r_+ + r_-$, where r_+ and r_- are the radius of the cation and anion respectively.
- N_A is the Avogadro's constant.
- z_+ and z_- are the are the charge number for the cation and anions.
- e is the fundamental charge
- ϵ_0 is the vacuum permittivity (dielectric constant at vacuum).
- d^* is a constant that represents the repulsion between ions at short range.
- A is the Mandelug constant and depends on the relative distribution of ions (structure).

The ΔH° can be seem as the enthalpy change accompanying the formation of a gas of ions from the solid and can be represented used a Termochemical equation as :

$$MX(s) \quad \rightarrow \quad M^+(g) + X^-(g) \qquad \Delta H^\circ$$

where

- $MX(s)$ is the ionic compound in the solid state.
- $M^+(g)$ and $X^-(g)$ are the cation and the anion in the gas state respectively.
- ΔH° is the energy needed to separate the atoms, hence, ΔH° is positive.

5.1.1 Application of the Born-Mayer equation for Choline Chloride

We use the ionic radius of the Na, Cl and Choline(Ch) given in the table 3 to compare the lattice enthalpy of ChCl and NaCl using the Born-Mayer equation :

$\Delta H^{\circ}_{NaCl} = 7.60\ x\ 10^5 Jmol^{-1}$

The experimental lattice enthalpy for NaCl is 786 $kJ\ mol^{-1}$ and is obtained using the Born-Haber cycle, comparing with the Born-Mayer equation we get that the error is less than 5%.

Using the Born-Mayer equation for ChCl we obtain :

$\Delta H^{\circ}_{ChCl} = 5.18\ x\ 10^5 Jmol^{-1}$

Comparing the lattice enthalpy of ChCl and NaCl, the next relation is derived :

$$\Delta H^{\circ}_{ChCl} \approx \frac{2}{3}\Delta H^{\circ}_{NaCl}$$

5.2 Competitive contributions for enthalpy in coulombic systems

The Enthalpy change of solution ΔH_{sol} relates the lattice enthalpy and the hydration enthalpy [7][5], which is a special case of the dissolution enthalpy (solvation enthalpy) where the solvent is water, the enthalpy change of solution is given by :

$$\Delta H^{\circ}_{sol} = \Delta H^{\circ}_{lattice} + \Delta H^{\circ}_{hyd}$$

$$\Delta H^{\circ}_{sol} = \Delta H^{\circ}_{lattice} + \Delta H^{\circ}_{+hyd} + \Delta H^{\circ}_{-hyd}$$

In which ΔH°_{+hyd} and ΔH°_{-hyd} are the hydration enthalpies for the cation

and the anion respectively.

The hydration is a process in which cations and anions are surrounded by water molecules.

The hydration enthalpy is the amount of energy liberated when one mole of ions are hydrated. This reaction is exotermic so the change of enthalpy is negative [7][5][16].

There are a lot of tables with experimental Hydration energies for simple cations and ions, the values of Na and Cl where obtained in this manner, but for choline (ChCl) we used an approximate expression obtained in [17].

The Hydration energies for Na and Cl are $-444\ kJ\ mol^{-1}$ and $-340\ kJ\ mol^{-1}$ respectively [5].

Using this with the lattice enthalpy we obtain:

$$\Delta H^{\circ}_{sol} = 786\ kJ\ mol^{-1} - (444\ kJ\ mol^{-1}\ +\ 340\ kJ\ mol^{-1})$$

$$\Delta H^{\circ}_{sol} = 4\ kJ\ mol^{-1}$$

For ChCl the hydration enthalpy is given by [17] :

$$\Delta H^{\circ}_{Hyd} = \frac{-700z}{r + 0.85}\ kJ\ mol^{-1}$$

In which z is the charge number of the cation and r is the ionic radius, this model give low values of $-\Delta H^{\circ}_{Hyd}$ because does not take int account the polarizability of the ions.

$$\Delta H^{\circ}_{Hyd} = -208.96\ kJ\ mol^{-1}$$

Using this result with the hydration enthalpy of the chlorine and the lattice enthalpy of the ChCl we obtained :

$$\Delta H^{\circ}_{sol} = 518\ kJ\ mol^{-1} - (208.96\ kJ\ mol^{-1} + 340\ kJ\ mol^{-1})$$

$\Delta H^{\circ}_{sol} = -30.96\ kJ\ mol^{-1}$

This result is much smaller than the obtained for NaCl, which indicates the facility of solvation for the ChCl in water.

5.3 Solvation Enthalpy: comparison between Urea and Etg

We used the Born equation for the Gibbs free energy [16] (standard molar) of solvation to make a comparison between Urea and Etg, this equation is given by :

$$\Delta G^{\circ}_{solvation} = N_A \left(\frac{z_+^2 e^2}{8\pi\epsilon_0 r_+} + \frac{z_-^2 e^2}{8\pi\epsilon_0 r_-} \right) \left(1 - \frac{1}{\epsilon_r} \right)$$

- r_+ and r_- are the radius of the cation and anion respectively.
- N_A is the Avogadro's constant.
- z_+ and z_- are the are the charge number for the cation and anions.
- e is the fundamental charge
- ϵ_0 is the vacuum permittivity (dielectric constant at vacuum).
- ϵ_r is the relative permittivity of the medium (dielectric constant of the medium).

We related this equation to the enthalpy, using the equation of state of ΔG.

$$\Delta G = \Delta H + T\Delta S$$

Substituting the Born equation in the equation of state we have :

$$\Delta H^{\circ}_{solvation} = \Delta G^{\circ}_{solvation} - T\Delta S^{\circ}_{solvation}$$

Making an approximation for this equation, setting T=0 like in the Born-Mayer equation give us :

$$\Delta H^{\circ}_{solvation} \approx N_A \left(\frac{z_+^2 e^2}{8\pi\epsilon_0 r_+} + \frac{z_-^2 e^2}{8\pi\epsilon_0 r_-} \right) \left(1 - \frac{1}{\epsilon_r} \right)$$

With this equation we can compare the capacity of disrupt the lattice enthalpy caused by a solvent, in this case Urea and Etg.

The relative permittivity of water [10], urea [3], Etg [10] and the ΔH°_{sol} obtained using the Born equation are in the next table.

Compounds	Relative permittivity at room temperature	ΔH°_{sol}
Urea	$\approx 3.5 - 8$	$-529\ kJ\ mol^{-1}$
Etg	≈ 37	$-644\ kJ\ mol^{-1}$
Water	≈ 80	$-653\ kJ\ mol^{-1}$

Table 14: Comparison between the enthalpy of solvation and the dielectric constant

The dielectric constant was employed to compare the ΔH°_{sol} for the ChCl using Urea, Etg and water as solvents.

This approximation gives greater values of $-\Delta H^{\circ}_{solvation}$, because the temperature in which this reactions occurs is not T=0 K, so the term $T\Delta S$ would diminish the value of $-\Delta H^{\circ}_{solvation}$, but this approximation can give us a starting point to analyze the effect of ϵ_r in the diminishing of the lattice enthalpy and the enthalpy of solution.

We can see than the power to disrupt the lattice energy is greater when ϵ_r is greater.

5.4 Limitations of the model

We have shown some of the advantages and made some quantitative analysis of the proposed model, but there are some disadvantages to take in account when this model is used.

For complex ions like choline chloride (organic ions), which can have more than one functional groups, this model gives a raw approximation for the interactions of this groups. Hence, the polarization of the molecules is not taken in account, this can lead to have smaller values for the $-\Delta H_{hyd}$ or $-\Delta H_{solvation}$.

Another problem is that we are treating the solvents like a continue with a dielectric constant ϵ, but in reality the effects of the interaction between the molecules of solvent are relevant.

6 Screening of the electrostatic interaction

Let us summarize the principal results obtained in the previous sections. We start by analyzing the results of the choline chloride salt and then we discuss the principal effects when the ethylene glycol or urea is added. The main aim of such discussion is to detect some general patterns which allows us to distinct physical insights that qualitative explain the differences among IL and DES.

The first characteristic that we can notice in the $ChCl$ salt is the "phase shifting" that take place between g_{+-} against g_{++} and g_{--} (see Fig 8), this "phase shifting" is one of the principal features that characterize ionic liquids like molten salts, electrolytes and liquid metals, in which the main interaction is the Coulombic interaction between the ions [15][20].

The main studied molten salts are the alkali halides, in which the best and more known example is sodium chloride ($NaCl$) [15], at this moment, comparisons between $NaCl$ and $ChCl$ will be very illustrative.

From Fig. 17 and 13 we observe that, for the systems studied, the presence of either Etg or Urea results in a higher mobility compared with the salt. Hence, it is possible to conclude that the DES are liquid at room temperature while the ChCl is solid.

The "phase shifting" also called "charge ordering" implies that the long-range electrostatic interactions promotes the pairing of the ions.

If we analyze g_{+-} in the $ChCl$ salt we can observe that, there is an attractive interaction between the cation and the anion ,hence, these ions get as close as possible until they are repelled by their ionic diameters.

This kind of interaction can show us the role of the ionic diameters in the package effect. For simplification we take the ionic diameters as hard spheres with out polarization effects.

On the other hand, if we analyze g_{++} and g_{--} in the $ChCl$ salt we can observe that, there is a repulsive interaction between the ions (because they have same charge), this kind of interaction can show us the Coulombic force.

If we join both interactions, Coulombic and package effect (diameter of the particles), we can give an explanation for the "change ordering" effect.

First we consider a central ion, this ion would be surrounded by counter-ions, forming like a shell, the distance and the number of counter ions would be determined by the ionic diameter, this shell surrounding the central ion would be surrounding by other shell of counter-ions, but in this case the central ion try to repel this second shell because, they have the same charge so, now we have a competition between forces, in one side we have the Coulombic interaction that attract the ions and counter ions to form a shell structure, also the shells of the same charge try to repel each other, by the other hand, we have the ionic diameter which determines the distance between adjacent shells.

This phenomena is characteristic of Coulombic systems, like ionic liquids, in which the components not just try to achieve charge neutrality in bulk but in a microscopic scale also. This is the reason of forming shells of counter-ions around ions, in a microscopic scale the system try to neutralize itself and this behavior takes the system to "screen" the Coulombic potential to achieve bulk neutrality [15].

On the other hand, a remarkable difference in the size of the cation is observed for ChCl compared with NaCl. In the ChCl case we have that the cation is ≈ 1.3 times larger that the anion. The application of the Born-Mayer formula, using such size asymmetry, results in the relation $\Delta H^{\circ}_{ChCl} \approx \frac{2}{3}\Delta H^{\circ}_{NaCl}$

The lattice enthalpy estimates the amount of energy necessary to form ionic bonds between cations and anions. Hence, a lower value of lattice enthalpy means that the $ChCl$ ionic structure can be "separated" easily (the ionic bonds need less energy to be disrupted) either by increasing temperature to reach the melting point or by solvation effects. In this manner, it is possible to explain the lowering of the melting point of the ChCl ($\approx 575\ K$) compared with the NaCl ($\approx 1273\ K$).

6.1 Screened electrostatic interactions in ChCl-Ure and ChCl-Etg

The observations presented previously show that the presence of the hydrogen-bond donor has enormous consequences in the stability of the crystalline order of the ChCl salt. At least for the two DES studied, we can observe that the adding of such compounds reduce the stability of the crystalline phase by the decreasing of the electrostatic interactions between the ions.
The calculations contained in Table 14 show that the ChCl salt has a higher value of the lattice enthalpy compared with the ChCl-Urea and ChCl-Etg mixtures.

From the thermochemical calculations we observe that the $H^{\circ}_{solvation}$,

obtained with the Born equation, of the urea is bigger than the lattice enthalpy of ChCl. Thus, the urea allows the separation of the ions in an easier manner, diminishing the crystalline structure of the ChCl crystal. The net effect of the urea in the ChCl salt is the disruption and disturbing of the crystalline structure, principally, affecting the interaction between cations and anions. The structural properties also show a decreasing of the effective interaction when the urea is added.

As shown in fig 12 and 16 an overall reduction of the main peak of g_{+-} and g_{++}, which is a clear evidence of the decrease of the interactions between ions.

If we check the urea interactions in the results, we can noticed that the g_{U-} first peak distance is less than the g_{+-} first main peak, and the g_{+U} is also at less distance that g_{+-} second main peak. So, we can deduce that the urea molecule competes with the $CHL - Cl$ interaction, stacking up amid the CHL^+ and Cl^+ ions, diminishing the packing effect between them.

We can also observe in the MSD that the diffusion was slightly increased in the ChCl-Urea mixture.

The distances of the main and second peaks of g_{+-},g_{++} and g_{--} remains the same in the ChCl-Urea mixture compared with the $ChCl$ salt.

With this information, we can infer that the urea just affects the package structure of $ChCl$ in the mixture, diminishing the number of interaction between the ions and counter-ions of $ChCl$ but remaining the range of interaction, keeping the distance among counter-ions shells.

Now we analyzed the ETG effect when interact with $ChCl$. One of the principal features that we can notice in the $ChCl - Etg$ mixture is the distance of separation between the Cl^- anions, this can be noticed comparing the g_{--} of $ChCl - Etg$ mixture against the g_{--} of the $ChCl$ salt.

Unlike urea, the distance increasing ($\approx 0.125\ nm$) between the Cl^- anions lead to a more space for the CHL^+ and ETG molecules to move, with a decrease of the Coulombic force and losing the crystalline structure that

ones had the $ChCl$ salt.

Analyzing the results, we can observe that g_{E-} main peak is at less distance than the g_{+-} first main and second (little bump) main peaks. Therefore the increased anion separation, is caused by the increased in the ETG interaction with Cl^-, causing a more fluid state where the CHL^+ and ETG can diffuse, this is supported by the MSD results, that shows a huge increase in the diffusion of CHL^+, Cl^- and ETG in the $ChCl - Etg$ mixture.

In the termochemical view we observe that the $H^\circ_{solvation}$ of the Etg is much bigger than the lattice enthalpy of ChCl, bigger than urea even, so, the Etg can separate the ions with much strong that urea did and diminishing the crystalline structure of the ChCl in a greater way.

In resume, the effects of urea and ETG with $ChCl$ are similar to the effect of water with $NaCl$, dissociating the anions and cations, and disrupting the crystalline structure of the system and forming structures like "Solvation shells".

The main difference is that, the $ChCl$ lattice have lower energy compared with $NaCl$ therefore, $ChCl$ needs a compound with lower relative permittivity (dielectric constant) to diminish the Coulombic force and dissociate the ions.

In this case Etg and Urea would be the solvents that dissociate the ions in the ChCl salt, but the relative permittivity of Etg is greater than urea so, the solvation effect is stronger.

7 Perspectives

The results presented previously, represent an attempt for obtaining physical insights which explain the diminution of the melting point in DES. Despite our results show that the presence of the hydrogen-bond donor (Urea o Etg) reduces the electrostatic interactions between ions. As a consequence, the stability of the crystalline phase is decreased. However, we used the most simple models in order to have a first approach to the problem. There exist several improvements to our models which can be implemented in the near future. Examples of such kind of improvements are presented in the following.

First, the assumption of a hard sphere model, we can improve that using an effective radius, this effective radius can take in account the polarity of the molecules, giving an effective radius depending of the polar interactions between the solvent and the solute.

An other improving could be diminishing or increasing the charge of the ions giving them fractional charges depending of the solvent and solute interactions.

To obtain a better results of the capacity of a solvent to disrupt a ionic lattice, we can take the solvent molecules as a neutral hard sphere and include a diminishing of the ionic charge, depending on the dielectric constant ϵ.

In addition, it is possible to develop an effective theory which reduce the contribution of the hydrogen-bond donor to an overall reduction of the electrostatic interactions. Such kind of models already exist in the context of electrolytic solutions as NaCl-H_2O.

8 Conclusions

Two Deep Eutectic Solvents (DES) and an Ionic Liquid (IL) were analyzed using a MD simulation, their MSD and RDF were obtained in the aim to discover the causes of the freezing point decreasing of these DES at room temperature. The results given by the MD simulation were complemented with a thermochemical analysis of the DES and the IL, in which the lattice enthalpy of the IL and NaCl, both in a crystalline state, were compared. Also, the enthalpy of solution of the DES was obtained and compared with the relative permittivity (dielectric constant) of the Urea, Etg and Water.

As a conclusion of this analysis we can declare that the freezing point depression in the DES studied is caused because of the solvation generated by the Urea and Etg molecules that disrupt the lattice energy of the IL. The lattice enthalpy of the IL depends mainly on the ionic radius of the cation and anion. Hence the lattice enthalpy of the IL is diminished in a great way principally because of the big size of the choline molecule.

The intensity of the disruption depends on the dielectric constant ϵ of the solvent, Etg has bigger ϵ than urea so, the effects on the crystalline structure of the IL are stronger. Therefore we can relate the ϵ of the Etg with the great decreasing in the freezing point of the DES (Etg) compared with the DES (Urea).

9 Appendix

9.1 Physical concepts for molecular dynamics simulations

9.1.1 Verlet algorithm

In this section we will work with the physical concepts that are used in the simulation. First we can analyze the problem in the more general aspects, like the size of the system. We know that for a realistic simulation $\approx 10^{23}$ particles (the Avogadro's number) are needed, that's impossible to do because the information given by the simulation could not be analyzed, so the first approximation would be using a representative part of molecules. The number of representative molecules used should be enough to obtain statistical averages with low fluctuations, so we can obtain representative macroscopic properties of the system.

In our case we will use ≈ 1000 molecules, each one which 10 or 20 atoms for the simulation, so what can we do to obtain a bigger representative system with reliable representative macroscopic properties ? , and how can we minimize the edge effect (surface effect) of our system since is finite in extension ?

To overcome this situation we used Periodic Boundary Conditions or just PBD. We will explain how it works lately in the chapter, for now we should

know that we have a representative system to which we can measure representative macroscopic properties.
Now we have the representative system (in the next we just call it the system), the next part is to solve the equations of motion of the molecules, to do that we have to use the time dependent Schrödinger equation for all molecules in the system. In this case our molecules are to complex to do that so we need another approximation. We can analyze the distance between the molecules to know if quantum contributions are representative. The Thermal de Broglie wavelength Λ can tell us if we can use a classical approximation to the problem. If Λ is much smaller than the particle interdistance a we can consider a classical or Maxwell-Boltzman system.

$$\Lambda << a$$

Another consideration is the characteristic rotational temperature Θ_{rot}, which must be much smaller than the triple point temperature T_t of the molecule to neglect quantum contributions.

$$\Theta_{rot} << T_t$$

The explicit analysis of Λ and Θ are in [15].

Now that we know our system satisfy the last two conditions, and can be treated like a classical system, we need to solve the Newton's equation of motion for all the molecules in the system, that is to solve :

$$m\mathbf{a} = \mathbf{F} \quad for \quad N \quad particles$$

$$m^{[i]}\frac{d^2\mathbf{r}^{[i]}}{dt^2} = \mathbf{F}_i \quad for \quad i = 1, ..., N$$

where $m^{[i]}$ are the masses of the particles, $\mathbf{r}^{[i]}$ are the coordinates of the particles and $\mathbf{F}_i$ are the forces acting on the particle i.
To solve those equations for $\mathbf{r}^{[i]}$ we used Taylor series so :

$$\mathbf{r}^{[i]}(t) = \mathbf{r}^{[i]}(t_0) + \frac{d\mathbf{r}^{[i]}}{dt}\Big|_{t=t_0}(t-t_0) + \frac{d^2\mathbf{r}^{[i]}}{dt^2}\Big|_{t=t_0}\frac{(t-t_0)^2}{2!} + \frac{d^3\mathbf{r}^{[i]}}{dt^3}\Big|_{t=t_0}\frac{(t-t_0)^3}{3!} + O((t-t_0)^4)$$

$$for \quad i = 1, ..., N$$

where :

$$\frac{d\mathbf{r}^{[i]}}{dt} = \mathbf{v}^{[i]}$$
$$\frac{d^2\mathbf{r}^{[i]}}{dt^2} = \mathbf{a}^{[i]}$$

Now subtracting $\mathbf{r}^{[i]}(t_{k-1})$ of $\mathbf{r}^{[i]}(t_{k+1})$ we have :

$$\mathbf{r}^{[i]}(t_{k+1}) = 2\mathbf{r}^{[i]}(t_k) - \mathbf{r}^{[i]}(t_{k-1}) + \frac{\mathbf{F}^{[i]}(t_k)}{m^{[i]}}\Delta t^2$$
$$for \quad i = 1, ..., N \quad and \quad k = 0, ..., \tau$$

Now that we have the position of the particles in the time t_{k+1}, we need just to follow the algorithm shown in the figure 2.

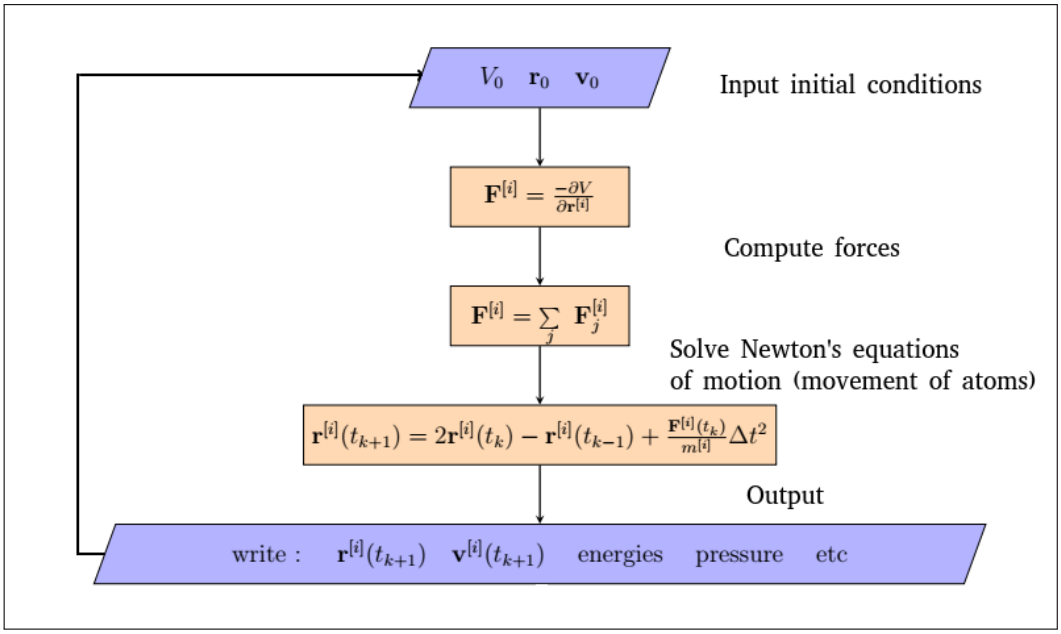

Figure 28: Verlet algorithm

which is the Verlet algorithm, a more detailed view is in [4][11][14].

9.1.2 Interatomic potentials

As we can see in the diagram the force is given by $\frac{-\partial V}{\partial \mathbf{r}}$ where V is the potential energy of the system.

The form of this potential can be divided in covalent bond interactions called bonded which are separated in bonds, angles and torsions or non-bonded interactions which are electrostatic long range and Van der Waals interactions.

In molecular modeling the potential energy of the system is called force field, for our simulation we used the AMBER 94 (Assisted Model Building with Energy Refinement) force field [8], and the functional form of this force field has the form :

$$V\left(r^N\right) = \sum_{bonds} k_b(l - l_0)^2 + \sum_{angles} k_a(\theta - \theta_0)^2$$
$$+ \sum_{torsions} \sum_{n} \frac{1}{2} V_n[1 + cos(n\omega - \gamma)]$$
$$+ \sum_{j=1} \sum_{i=j+1} f_{ij} \left\{ \epsilon_{ij} \left[\left(\frac{r_{0ij}}{r_{ij}} \right)^{12} - \left(\frac{r_{0ij}}{r_{ij}} \right)^{6} \right] + \frac{q_i q_j}{4\pi\epsilon_0 r_{ij}} \right\}$$

The first term of the equation indicates the energy between covalent bonded atoms. This is an harmonic force like an ideal spring.

The second term indicates the energy due to the geometry of electron orbitals forming covalent bonding. This is also an harmonic force like an ideal spring.

The third term indicates the energy for twisting bonds due to a bond order.

The forth term indicates the energy due to Van der Waals and electrostatic energies which represents the non-bonded energy between all atom pairs.

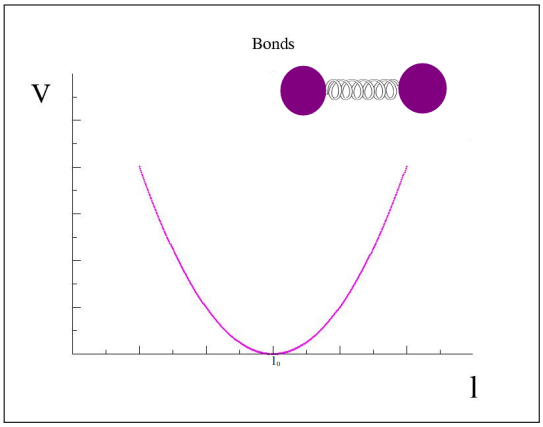

(a) bonds

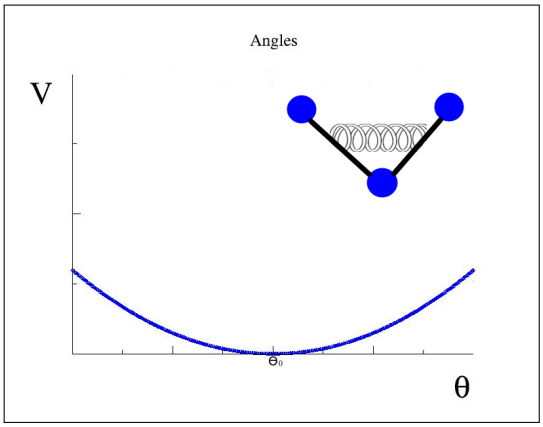

(b) angles

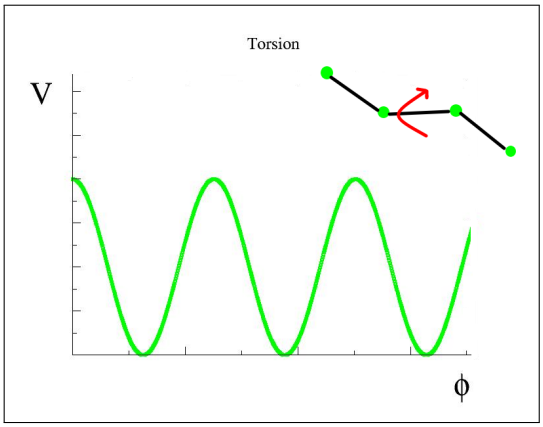

(c) torsion

Figure 29: Covalent interactions

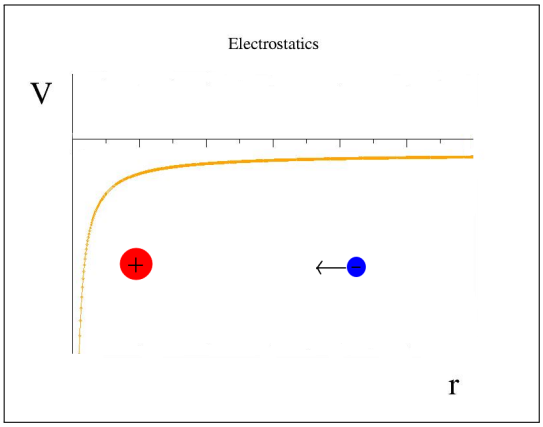

(a) Electrostatic interaction

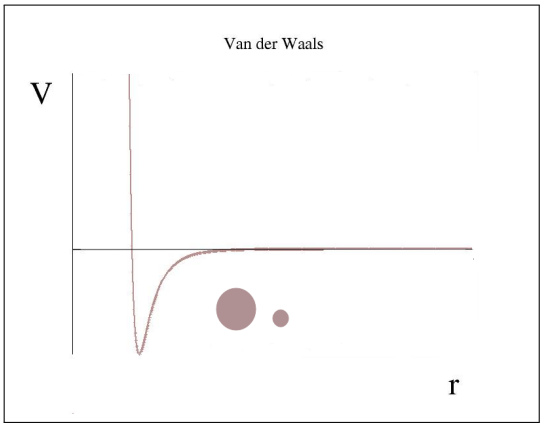

(b) Van der Waals interaction

Figure 30: Non-covalent interaction

9.1.3 Periodic boundary conditions

In systems with few particles ($\approx$ 1000 in this case) the surface effects are of great importance, if we want to study the bulk system without surface effects we can used a trick to expand and make a bigger system without an increment of the number of particles so, saving computational cost, this "trick" is called Periodic Boundary Conditions or just PBC [4][14].

First we take all the N particles in the system, and put them inside a finite volume V, this would be our primary cell, and then make identical copies of the primary cell (image cells) to form a lattice. In the figure 5 we can see an example of a 2-dimensional system. In this lattice from the x-axis if a particle go out from the right side, it will return from the left size, the same happened if go out from the left side, it will return from the right side, then the same idea can be applied to the y-axis and z-axis (if there is a 3-dimensional system), hence we can keep a constant density of particles and in all cases the momentum of the particles are conserved [4].

To measure properties of the system we just need to store the positions and momentum of the N atoms in the primary cell, if we need the positions or momentum of the images, they can be computed by coordinate transformations [14].

Despite PDB can be used to avoid some surface effects in the simulation, this method can lead to temporal periodicity problems, which could affect time dependent properties like correlation functions in equilibrium systems [14].

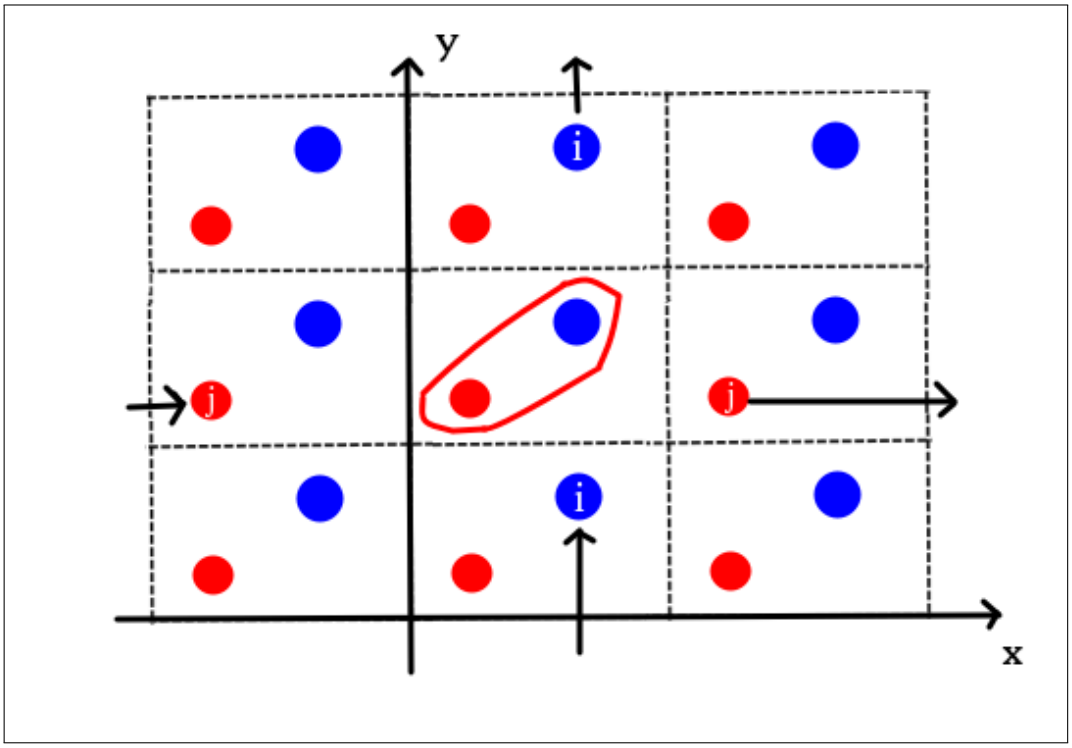

Figure 31: 2-D system PBC

9.1.4 Statistical ensembles

Another tool in the making of molecular dynamic simulations is statistical mechanics, in which the concept of statistical ensembles is fundamental.

To understand this, we will use the Gibbs approach to mechanical statistics to describe an ensemble and then explain the ensembles used in the simulation, more detailed information is given in [15][13][19].

A statistical ensemble is a virtual collection consisting of a large number of systems, each of one represent a possible state of the real system, considering all the states of the system at once. The states of the system have a probability distribution that obey the principle of equal a priori

probability. That is, the probability to be in any possible state is the same for an isolated system.

To obtain the thermodynamic properties of the system, we average over all the members of the ensemble of a mechanical (pressure, energy, volume) or non-mechanical (entropy, free energy) property, we do that taking in count the equal a priori probability.

The difference between mechanical and non-mechanical properties is that non-mechanical properties involve the concept of temperature and the mechanical not.

One characteristic of an statistical ensemble is stationarity. There is not changing over time, and we can say that the statistical ensemble is in statistical equilibrium.

The statistical ensembles that we used in the simulation were:

Microcanonical ensemble (NVE) : is a statistical ensemble where the number of particles and the temperature are fixed in a container with fixed volume and adiabatic walls, so the system is completely isolated and can not interchange energy and particles with the exterior.

Canonical ensemble (NVT) : is a statistical ensemble where the number of particles is fixed but the energy of the system is not, the container has a fixed volume and diathermic walls thus can exchange energy with the exterior. We can say that the container is in a thermal contact with a heat bath in which the temperature will be the same when thermal equilibrium is reached.

Isothermal-isobaric ensemble (NPT) : this statistical ensemble is similar to NVT ensemble but the volume of the container is not fixed so the applied pressure can be constant in thermal equilibrium.

Grand canonical ensemble (μVT) : in this ensemble the number of particles and the energy are not fixed so we can consider it as an open system in contact with a reservoir (thermal, chemical, etc.), where the chemical potential and the temperature are fixed.

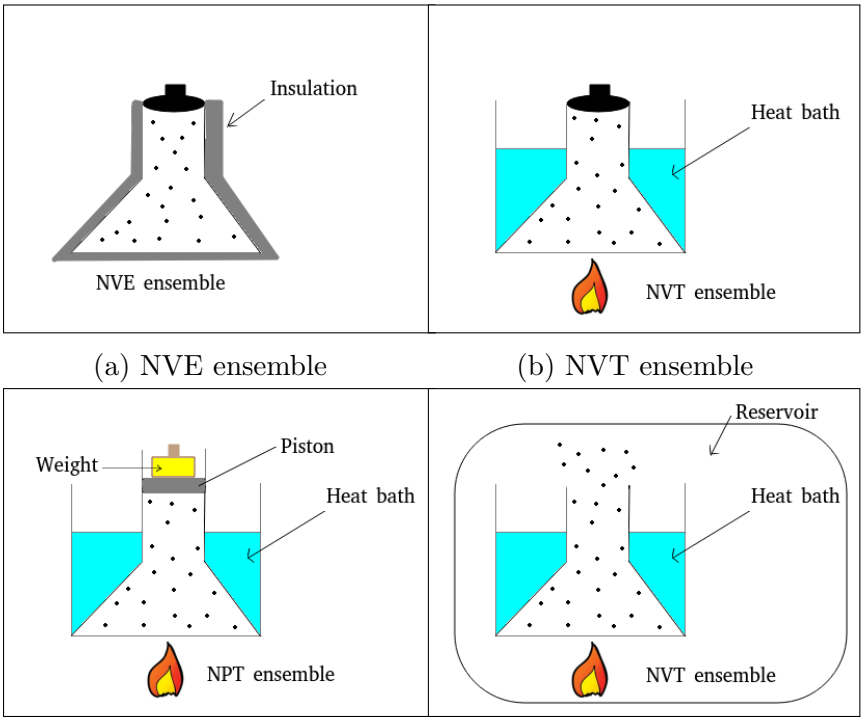

(a) NVE ensemble (b) NVT ensemble

(c) NPT ensemble (d) μVT ensemble

Figure 32: Statistical ensembles used in the simulation

9.2 Radial distribution function

The radial distribution function $g(r)$, is a pair distribution function that show us the local structure of atoms in the system.

The $g(r)$ is proportional to the probability of finding two atoms separated by a distance $r + \Delta r$.

The Fourier transform of $g(r)$ called structure factor ($S(k)$) can be obtained experimentally using x-ray or neutron diffraction hence, we can relate $g(r)$ with the structure and organization of atoms obtained experimentally.
The last definitions were taken from [4][11][14].

The $g(r)$ can be obtained analytically, examples are the hypernetted chain and Percus-Yevick ecuations [15][19], but we will derive the expression used in MD simulations, actually is easier to obtain the $g(r)$ from simulations because MD simulations provide the trajectories of all atoms as a function of time.

So, we can obtain an expression that can be used for MD simulations, using a derivation from [14] we have :

First the radial distribution function is defined by :

$$\rho g(\mathbf{r}) = \frac{1}{N} \left\langle \sum_{i}^{N} \sum_{j \neq i} \delta \left[\mathbf{r} - \mathbf{r}_{ij} \right] \right\rangle$$

In this equation the angular brackets represents a time average, δ is the Dirac delta, $\mathbf{r}_{ij}$ is the vector between the center of atoms i and j , N is the total number of atoms and $\rho = \dfrac{N}{V}$ is the number density.

If we have an homogeneous and uniform substance, the structural arrangement of the atoms depends only on the distance r between atoms and is independent of the orientation of the separation vector $\mathbf{r}$, so we can made a simplification

$$\rho g(r) = \frac{1}{N} \left\langle \sum_{i}^{N} \sum_{j \neq i}^{N} \delta \left[r - r_{ij} \right] \right\rangle$$

The distance r_{ij} is invariant under interchange of labels i ans j , hence only

$\frac{1}{2}$ of the terms are unique. Therefore we write

$$\rho g(r) = \frac{2}{N} \left\langle \sum_{i}^{N} \sum_{j<i}^{N} \delta \left[r - r_{ij} \right] \right\rangle$$

The next step is $g(r)$ normalization, so we integrate over all possible separations of two atoms

$$\rho \int g(r) d\mathbf{r} = \frac{2}{N} \left\langle \sum_{i}^{N} \sum_{j<i}^{N} \int \delta \left[r - r_{ij} \right] d\mathbf{r} \right\rangle \qquad (*)$$

Using Dirac delta properties

$$\delta \left[r - r_{ij} \right] = \begin{cases} \infty & \text{if center of atom } ij \text{ is located at } r_{ij}. \\ 0 & \text{if center of atom } ij \text{ is not located at } r_{ij}. \end{cases}$$

$$\int_{a}^{b} \delta \left[r - r_{ij} \right] d\mathbf{r} = 1$$

Now we have

$$\rho \int g(r) d\mathbf{r} = \frac{N}{N}(N-1) \approx N$$

In this equation we can see that if we take one atom and count the other atoms in the system, we find $N - 1$ other atoms.

We can take this equation to make a probabilistic interpretation of $g(r)$.

$$\frac{\rho}{N-1}g(r)V(r,\Delta r) = \begin{cases} \text{Probability that an atomic center lies in a spherical} \\ \text{shell of radius } r \text{ and thickness } \Delta r \text{ with the shell} \\ \text{centered on another atom.} \end{cases}$$

In this probabilistic approach of the $g(r)$ we can see how the presence of an atom influences the position of neighboring atoms on a time average.

For a separation lower than the atomic diameter in a hard sphere system, $g(r) = 0$ because they can not overlap, for large separations in fluids an atom do not have influence on the position of another atom, so at long distances the density will be uniform and then $g(r) = 1$.

Now we can use equation $(*)$ but using a small and finite shell of thickness Δr to obtain an expression for evaluating $g(r)$ from the simulation.

$$\rho \sum_{\Delta r} g(r)V\left(r,\Delta r\right) = \frac{2}{N}\sum_{\Delta r}\left\langle \sum_{i}^{N}\sum_{j<i}^{N}\int \delta\left[r - r_{ij}\right]\Delta\mathbf{r}\right\rangle$$

The double sum is a counting operation, and is analogous to

$$\sum_{i}^{N}\sum_{j<i}^{N}\int \delta\left[r - r_{ij}\right]\Delta\mathbf{r} = N\left(r,\Delta r\right)$$

Here $N\left(r,\Delta r\right)$ is the number of atoms found in a spherical shell of radius r and thickness Δr, with the shell centered on another atom. Now we substitute this equation to the expression for g(r):

$$g(r) = \frac{\left\langle N\left(r,\Delta r\right)\right\rangle}{\frac{1}{2}N\rho V\left(r,\Delta r\right)}$$

If we write the time average explicitly over a total M times steps, where t_k is the time step, we have

$$g(r) = \frac{\sum_{k=1}^{M} N_k\left(r, \Delta r\right)}{M\left(\frac{1}{2}N\right)\rho V\left(r, \Delta r\right)}$$

Where N_k is the counting operation at time t_k. That is the general form used in MD simulations.

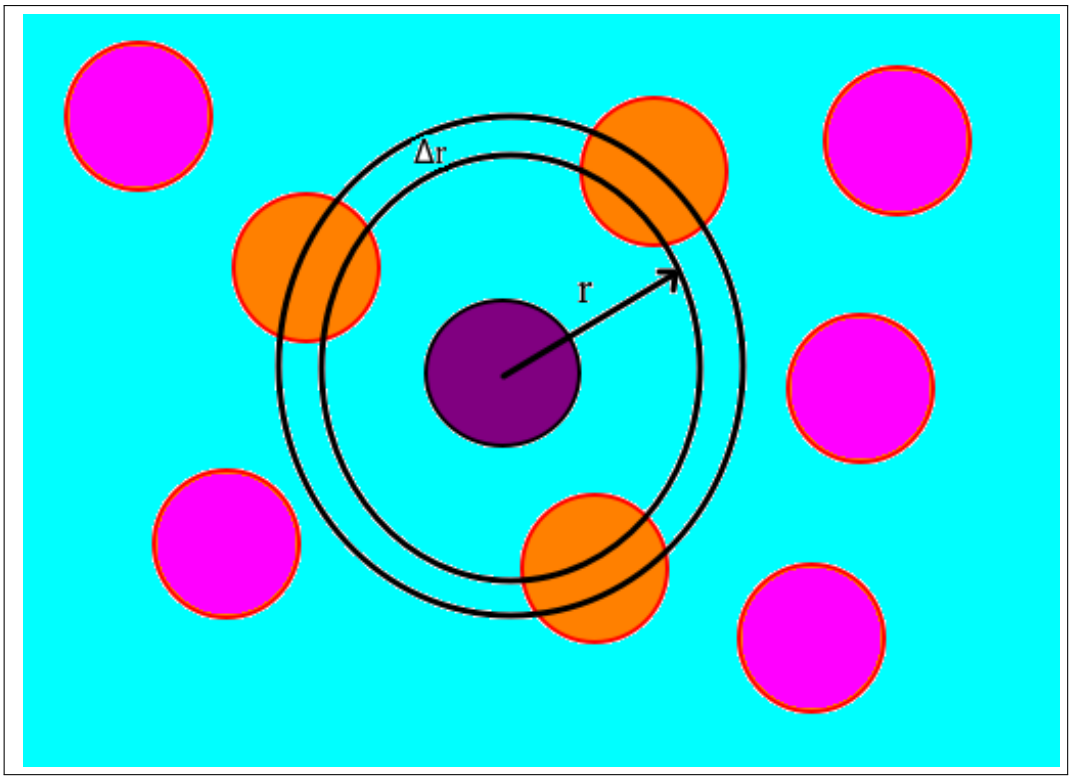

Figure 33: 2-D system g(r)

9.3 Mean square displacement

The mean square displacement (MSD) measures the deviation of the position of a random motion particle with respect a reference position over time. It can be seen as how much the particle moves or "explores" the system.

We will derive the (MSD) using the generalized Einstein equation in one dimension [14].

We start using the Fick's law to describe the diffusion process :

$$N(x,t)\frac{\partial x}{\partial t} = -D\frac{\partial N}{\partial x}$$

where $N(x,t)$ is the number of particles per length, $\dfrac{\partial x}{\partial t}$ is the local velocity, hence, $N(x,t)\dfrac{\partial x}{\partial t}$ is the flux of particles per length and D is the diffusion coefficient.

From a material balance on a differential element of fluid, we obtain the equation of continuity of mass.

$$\frac{\partial N}{\partial t} = D\frac{\partial^2 N}{\partial x^2}$$

The diffusion equation can be solved for the temporal and spatial evolution of $N(x,t)$, for a set of initial conditions.

If at time $t = 0$, N_0 atoms were concentrated at the origin $x = 0$, the solution for the diffusion equation is

$$N(x,t) = \frac{N_0}{2\sqrt{\pi Dt}} \exp\left[\frac{-x^2}{4Dt}\right]$$

This equation tell us that at any time $t > 0$, the atoms are in a Gaussian spatial distribution around the origin, and as time evolves, the atoms diffuse away from the origin, and when the time is very large, $t \to \infty$, the Gaussian collapse.

At any time $t > 0$ the second moment of the distribution gives the MSD of the atoms

$$\left\langle [x(t) - x(0)]^2 \right\rangle = \frac{1}{N_0} \int x^2 N(x,t) dx$$

If we substitute $N(x,t)$ in this equation and make the integration, we find that the MSD is related to the diffusion coefficient D.

$$\left\langle [x(t) - x(0)]^2 \right\rangle = 2Dt$$

If we do that for three dimensions we have

$$\left\langle [r(t) - r(0)]^2 \right\rangle = 6Dt$$

This equation is applied when the time t is large compared to the average time between collisions of atoms, so we have

$$\lim_{t\to\infty} \quad \frac{\left\langle [r(t) - r(0)]^2 \right\rangle}{6t} = D \qquad (\Delta)$$

Another way to obtain the MSD is using the Green-Kubo relation [14], this can be calculated from the velocity auto-correlation function and for one dimension system have the form

$$\lim_{t\to\infty} \frac{\left\langle [x(t) - x(0)]^2 \right\rangle}{2t} = \int_0^\infty d\tau \, \langle v(\tau) v(0) \rangle$$

The self-diffusion coefficient can be obtained rewriting the equation (Δ)

$$D = \frac{1}{6N} \lim_{t\to\infty} \frac{d}{dt} \left\langle \sum_i^N [\mathbf{r}_i(t) - \mathbf{r}_i(0)]^2 \right\rangle$$

This equation show us that D is proportional to the slope of the mean-square displacement at long times.

The self-diffusion coefficient taking the Green-Kubo relation can be written as

$$D = \int_0^\infty d\tau \, \langle v(\tau) v(0) \rangle$$

9.4 Thermodynamic review

Some thermodynamic concepts have been used to understand the physical changes on a macroscopical way of view, generally changes of energy are use to describe a phenomena in a system, but in this case changes of enthalpy were used, which give us a better and simpler way to understand phenomena like lattice disruption and ionic solvation.

We define the change of enthalpy ΔH in a simple words, as the heat transfer at constant pressure, in which an endthermic process implies a positive change of enthalpy $+\Delta H$, an and exothermic process implies a negative change of enthalpy $-\Delta H$ [5].

For the calculations we used the 'Standard Molar Enthalpies of Formation' denoted by ΔH°. The standard state of an element or compound is the physical state in which it exist at 1 bar of pressure and a specified temperature [7][5]. The enthalpy of a system can be represented as an equation of state, so we represent ΔH° as :

$$\Delta H^\circ = \Delta U^\circ + p\Delta V^\circ$$

In which U is the internal energy, p the pressure and V the volume of the system, the product $p\Delta V$ represents the work that is applied to the system and is related to the work necessary for the creation of space in the system, for the standard state we have that in a reaction

$$p\Delta V^\circ << \Delta U^\circ$$

hence we have that the change of enthalpy is approximately equal to the internal energy [7][5].

$$\Delta H^\circ \approx \Delta U^\circ$$

References

[1] Andrew P. Abbott et al. "Novel solvent properties of choline chloride/urea mixtures". In: *Chem. Commun.* (2003). DOI: 10.1039/B210714G.

[2] MJ Abraham et al. *the GROMACS Development Team (2014) GROMACS User Manual Version 5.0. 4*. 2015.

[3] Taher Alizadeh and Aezam Akbari. "A capacitive biosensor for ultra-trace level urea determination based on nano-sized urea-imprinted polymer receptors coated on graphite electrode surface". In: *Biosensors and Bioelectronics* (2013). DOI: https://doi.org/10.1016/j.bios.2012.12.043.

[4] M.P. Allen et al. *Computer Simulation of Liquids*. Clarendon Press, 1989.

[5] Peter Atkins, Julio De Paula, and James Keeler. *Atkins' physical chemistry*. Oxford university press, 2018.

[6] Peter Atkins and Tina Overton. *Shriver and Atkins' inorganic chemistry*. Oxford University Press, USA, 2010.

[7] Peter Atkins and Tina Overton. *Shriver and Atkins' inorganic chemistry*. Oxford University Press, USA, 2010.

[8] Wendy D. Cornell et al. "A Second Generation Force Field for the Simulation of Proteins, Nucleic Acids, and Organic Molecules". In: *Journal of the American Chemical Society* (1995). DOI: 10.1021/ja00124a002.

[9] R. Craveiro et al. "Properties and thermal behavior of natural deep eutectic solvents". In: *Journal of Molecular Liquids* (2016). DOI: https://doi.org/10.1016/j.molliq.2016.01.038.

[10] John Aurie Dean. *Lange's handbook of chemistry*. New york; London: McGraw-Hill, Inc., 1999.

[11] Daan Frenkel and Berend Smit. *Understanding molecular simulation: from algorithms to applications*. Elsevier, 2001.

[12] Gregorio García, Mert Atilhan, and Santiago Aparicio. "The impact of charges in force field parameterization for molecular dynamics simulations of deep eutectic solvents". In: *Journal of Molecular Liquids* (2015). DOI: https://doi.org/10.1016/j.molliq.2015.07.070.

[13] Josiah Willard Gibbs. "Elementary Principles of Statistical Mechanics". In: *Compare* (1902).

[14] JM Haile. "Molecular Dynamics Simulation Elementary Methods". In: ().

[15] Jean-Pierre Hansen and IR McDonald. *Theory of Simple Liquids*. Elsevier, 2006.

[16] Conrad L. Stanitski John W. Moore. *Chemistry the molecular science*. BROOKS/COLE CENGAGE Learning, 2011.

[17] David Arthur Johnson, David Arthur Johnson, and Eric Ed Johnson. *Some thermodynamic aspects of inorganic chemistry*. CUP Archive, 1982.

[18] JA Lemkul. *GROMACS Tutorial, Lysozyme in Water*. 2013.

[19] D.A. McQuarrie. *Statistical mechanics*. Harper & Row, 1975.

[20] George Papatheodorou. "STRUCTURE AND THERMODYNAMICS OF MOLTEN SALTS . In Advances in Electrochemistry". In: (2015). DOI: 10.13140/2.1.4424.5288.

[21] Sasha L. Perkins, Paul Painter, and Coray M. Colina. "Experimental and Computational Studies of Choline Chloride-Based Deep Eutectic Solvents". In: *Journal of Chemical & Engineering Data* (2014). DOI: 10.1021/je500520h.

[22] Sasha L. Perkins, Paul Painter, and Coray M. Colina. "Molecular Dynamic Simulations and Vibrational Analysis of an Ionic Liquid Analogue". In: *The Journal of Physical Chemistry B* (2013). DOI: 10.1021/jp404619x.

[23] Pedro E. Ramírez-González et al. "Effect of Ion Rigidity on Physical Properties of Ionic Liquids Studied by Molecular Dynamics Simulation". In: *The Journal of Physical Chemistry B* (2016). DOI: 10.1021/acs.jpcb.6b03379.

[24] Hui Sun et al. "Theoretical study on the structures and properties of mixtures of urea and choline chloride". In: *Journal of Molecular Modeling* (2013). DOI: 10.1007/s00894-013-1791-2.

[25] Baokun Tang and Kyung Ho Row. "Recent developments in deep eutectic solvents in chemical sciences". In: *Monatshefte für Chemie - Chemical Monthly* (2013).

[26] Qinghua Zhang et al. “Deep eutectic solvents: syntheses, properties and applications”. In: *Chem. Soc. Rev.* (2012). DOI: 10.1039/C2CS35178A.